DET NORSKE VIDENSKAPS-AKADEMI I OSLO

GEOFYSISKE PUBLIKASJONER
GEOPHYSICA NORVEGICA

Vol. XXVII. No. 4 April 1968

EIGIL HESSTVEDT

On the effect of vertical eddy transport on atmospheric composition in the mesosphere and lower thermosphere

OSLO 1968
UNIVERSITETSFORLAGET

GEOFYSISKE PUBLIKASJONER
GEOPHYSICA NORVEGICA
VOL. XXVII NO. 4

ON THE EFFECT OF VERTICAL EDDY TRANSPORT ON ATMOSPHERIC COMPOSITION IN THE MESOSPHERE AND LOWER THERMOSPHERE

By

Eigil Hesstvedt

FREMLAGT I VIDENSKAPS-AKADEMIETS MØTE DEN 17. NOVEMBER 1967

Summary. The composition of the mesosphere and lower thermosphere is studied theoretically in an oxygen-hydrogen atmosphere model. The effect of vertical eddy transport is shown to be considerable. With eddy diffusion coefficients ranging from about 4×10^5 cm^2/s at 65 km to about 7×10^6 cm^2/s at 100 km, water vapor is found to be a major hydrogen constituent up to levels well above the mesopause. Theoretical values for nightglow emission are computed. A theoretical value of the OH* emission was found to be 2300 kR with maximum emission at 88 km. For the atomic oxygen green line emission a mean value of about 100 R was obtained with maximum emission at 93 km.

1. Introduction. On the basis of their classical oxygen-hydrogen atmosphere model, Bates and Nicolet (1950) drew the first picture of the vertical distribution of oxygen and hydrogen components in the upper atmosphere. Since then the accuracy of the model has been increased by using improved data for temperature, pressure, reaction rates and ultraviolet solar radiation. In recent years, Hampson (1964, 1966) and Hunt (1966) have made the model still more complete by introducing some additional reactions which have turned out to be of importance, notably for ozone calculations in the stratosphere.

A study of the characteristic times for the various components, as a function of height, makes it clear that transport processes must play an important role. A convincing example is the effect of molecular diffusion upon the number densities of molecular oxygen in the thermosphere. But also eddy transport and mean motion will be important at certain levels, notably in the ozone layer and in the upper mesosphere and lower thermosphere.

It is the aim of this paper to eliminate some of the deficiencies of photochemical models in which transport processes are neglected by introducing vertical eddy trans-

port in the model. It is true that our knowledge of vertical eddy diffusion coefficients is poor, but in spite of this the model described below represents, for specific problems, a considerable improvement on models in which transport processes are neglected. As will be shown below, this becomes especially obvious for water vapor in the upper mesosphere and lower thermosphere.

2. Reaction rates. The reactions and reaction rates used in the present version of the oxygen-hydrogen atmosphere model are, with a few exceptions, the same as those used by HUNT (1966).

(1) $O(^3P)+O(^3P)+M\rightarrow O_2+M$ $k_1=2.7\times10^{-33}$ (REEVES, MANELLA and HARTECK, 1960)

(2) $O(^3P)+O_2+M\rightarrow O_3+M$ $k_2=8.2\times10^{-35}\exp(0.89/RT)$ (BENSON and AXWORTHY, 1965)

(3) $O(^3P)+O_3\rightarrow 2O_2$ $k_3=5.6\times10^{-11}\exp(-5.7/RT)$ (BENSON and AXWORTHY, 1965)

(4a) $O_2+h\nu\rightarrow O(^3P)+O(^3P)$ J_{2a} (1750 Å $<\lambda<$ 2424 Å)
(4b) $O_2+h\nu\rightarrow O(^3P)+O(^1D)$ J_{2b} ($\lambda<$ 1750 Å)
$\Big\}\ J_{2a}+J_{2b}=J_2$

(5a) $O_3+h\nu\rightarrow O(^3P)+O_2$ J_{3a} ($\lambda>$ 3100 Å)
(5b) $O_3+h\nu\rightarrow O(^1D)+O_2$ J_{3b} ($\lambda<$ 3100 Å)
$\Big\}\ J_{3a}+J_{3b}=J_3$

(6) $OH+O(^3P)\rightarrow H+O_2$ $k_6=5\times10^{-11}$ (KAUFMAN, 1964)

(7) $HO_2+O(^3P)\rightarrow OH+O_2$ $k_7=10^{-11}$ (KAUFMAN, 1964)

(8) $H+O_2+M\rightarrow HO_2+M$ $k_8=7.4\times10^{-32}$ (LARKIN and THRUSH, 1964)

(9) $H+O_3\rightarrow OH+O_2$ $k_9=2.6\times10^{-11}$ (KAUFMAN, 1964)

(10) $OH+HO_2\rightarrow H_2O+O_2$ $k_{10}=10^{-11}$ (KAUFMAN, 1964)

(11) $H_2O_2+h\nu\rightarrow 2\ OH$ $J_{H_2O_2}$ (1875 Å $<\lambda<$ 3825 Å)

(12) $O(^3P)+H_2O_2\rightarrow OH+HO_2$ $k_{12}=10^{-15}$ (FONER and HUDSON, 1962)

(13) $HO_2+HO_2\rightarrow H_2O_2+O_2$ $k_{13}=3\times10^{-12}$ (KAUFMAN, 1964)

(14) $OH+H_2O_2\rightarrow H_2O+HO_2$ $k_{14}=4\times10^{-13}$ (FONER and HUDSON, 1962)

(15) $OH+OH\rightarrow H_2O+O(^3P)$ $k_{15}=2.8\times10^{-12}$ (KAUFMAN, 1964)

(16) $H_2O+h\nu\rightarrow OH+H$ J_{H_2O} (1350 Å $<\lambda<$ 2375 Å + $Ly\alpha$)

(17) $H+HO_2\rightarrow H_2O+O(^3P)$ $k_{17}=2\times10^{-10}\exp(-4/RT)$ (BATES and NICOLET, 1950)

(18) $H+HO_2\rightarrow H_2+O_2$ $k_{18}=2\times10^{-13}$ (CLYNE and THRUSH, 1963)

(19) $H+H+M\rightarrow H_2+M$ $k_{19}=2.6\times10^{-32}$ (LARKIN and THRUSH, 1964)

(20) $O(^1D)+M\rightarrow O(^3P)+M$ $k_{20}=10^{-10}$ for $M=O_2$ (SCHIFF, 1967, and $k_{20}=2.2\times10^{-11}$ for $M=N_2$ DE MORE and RAPER, 1964)

(21) $O(^1D)+H_2\rightarrow OH+H$ $k_{21}=10^{-10}$ (HUNT, 1966)

(22) $O(^3P)+H_2\rightarrow OH+H$ $k_{22}=4.1\times10^{-11}\exp(-7.7/RT)$ (FENIMORE and JONES, 1958)

(23) $HO_2+O_3\rightarrow OH+2\ O_2$ $k_{23}=10^{-14}$ (HUNT, 1966)

(24)	$OH + O_3 \rightarrow HO_2 + O_2$	$k_{24} = 5 \times 10^{-13}$ (KAUFMAN, 1964)
(25)	$H + H_2O_2 \rightarrow H_2 + HO_2$	$k_{25} = 10^{-13}$ (FONER and HUDSON, 1962)
(26)	$H + O(^3P) + M \rightarrow OH + M$	$k_{26} = 8 \times 10^{-33}$ (BATES and NICOLET, 1950)
(27)	$H + O_3 \rightarrow HO_2 + O(^3P)$	$k_{27} = 2 \times 10^{-10} \exp(-4/RT)$ (BATES and NICOLET, 1950)
(28)	$H + O_2 \rightarrow OH + O(^3P)$	$k_{28} = 1 \times 10^{-9} \exp(-16.8/RT)$ (KAUFMAN, 1964)
(29)	$O(^1D) + H_2O \rightarrow 2\ OH$	$k_{29} = 10^{-11}$ (HUNT, 1966)
(30)	$H + HO_2 \rightarrow 2\ OH$	$k_{30} = 10^{-11}$ (KAUFMAN, 1964)
(31)	$H + OH + M \rightarrow H_2O + M$	$k_{31} = 2.5 \times 10^{-31}$ (KAUFMAN, 1964)
(32)	$O(^3P) + OH + M \rightarrow HO_2 + M$	$k_{32} = 1.4 \times 10^{-31}$ (PETERSEN and KRETSCHMER, 1960)
(33)	$H + OH \rightarrow H_2 + O(^3P)$	$k_{33} = 1.8 \times 10^{-12} \exp(-5.8/RT)$ (KAUFMAN, 1964)
(34)	$H_2 + OH \rightarrow H_2O + H$	$k_{34} = 10^{-10} \exp(-5.9/RT)$ (KAUFMAN, 1964)
(35)	$O(^1D) + O_3 \rightarrow 2\ O_2$	$k_{35} = 10^{-11}$ (FITZSIMMONS and BAIR, 1964)
(36)	$HO_2 + h\nu \rightarrow OH + O(^3P)$	J_{HO_2}

The units used are cm^3s^{-1} for two-body collisions, cm^6s^{-1} for three-body collisions, and s^{-1} for dissociation rates. The gas constant, R, is given in kcal/(mole · °K).

3. Dissociation rates. In the reaction scheme above the dissociations of O_2, O_3, H_2O, H_2O_2 and HO_2 are included. In the calculations of dissociation rates for O_2 and O_3 the usual data for solar radiation and absorption cross-sections were used, and consequently the resulting rates do not differ from those used by other authors. In the atmosphere important dissociation of H_2O may occur in two spectral regions, in the Lyα-region and in the interval 1350 to 2350 Å. For the Lyα-absorption $1.4 \times 10^{-17} cm^2$ was taken for the absorption cross-section (WATANABE, 1958). The intensity of the Lyα radiation was assumed to be 3.4×10^{11} photons/cm^2s (FRIEDMAN, 1961). Since the absorption cross-section of O_2 for this line is $1.1 \times 10^{-20} cm^2$, the Lyα dissociation rate for water vapor may be expressed as

$$J_{H_2O,Ly\alpha} = 4.7 \times 10^{-6} \exp(-1.1 \times 10^{-20} \cdot \Sigma_{O_2}) \tag{3.1}$$

where Σ_{O_2} is the optical thickness of O_2, given in particles pr. cm^2 column.

In the region 1350—1850 Å values for the absorption cross-section were taken from WATANABE (1958). Above 1850 Å the values of THOMPSON, HARTECK and REEVES (1963) were used to 1975 Å. For greater wave-lengths the contribution to the total dissociation rate is negligibly small.

Down to about 40 km J_{H_2O} is reduced by O_2-absorption. The effect of ozone absorption is very small and may be neglected. For optical thicknesses of O_2 smaller than $10^{20} cm^{-2}$ the dissociation rate for water vapor is only slightly influenced by O_2-absorption. For greater optical thicknesses the reduction proceeds rapidly.

Experimental determinations of absorption cross-sections of hydrogen peroxide have been reviewed by SCHUMB, GATTERFIELD and WENTWORTH (1955), and smoothed

values were read off their diagram. For HO_2 no data were available. In the present work the dissociation rates for H_2O_2 and HO_2 were assumed to be equal, as suggested by HUNT (1966).

Since dissociation of H_2O_2 is caused by radiation of longer wave-lengths, the dissociation rate is only slightly reduced down to 50 km.

Values for the dissociation rates are given in Table 1 for optical thicknesses of O_2 ranging from 10^{11} to 10^{22} cm^{-2}. The influence of O_3-absorption on the dissociation rates is negligible down to about 45 km. Approximate heights corresponding to a given thickness (vertical column) are given in the second column of the Table.

Table 1. *Dissociation rates as a function of optical thickness of O_2*

Optical thickness of O_2(cm^{-2})	Approximate height (km)	$J_{H_2O_2}$	J_{H_2O}	J_{2a}	J_{2b}	J_{3a}	J_{3b}
1×10^{17}	120	1.2×10^{-4}	1.0×10^{-5}	1.6×10^{-8}	2.9×10^{-6}	7.5×10^{-4}	8.4×10^{-3}
3×10^{17}	110	"	8.6×10^{-6}	"	1.4×10^{-6}	"	"
1×10^{18}	102	"	6.6×10^{-6}	"	3.9×10^{-7}	"	"
3×10^{18}	94	"	5.2×10^{-6}	1.5×10^{-8}	6.9×10^{-8}	"	"
1×10^{19}	87	"	4.4×10^{-6}	1.2×10^{-8}	2.3×10^{-9}	"	"
3×10^{19}	81	"	3.5×10^{-6}	8.9×10^{-9}	6.2×10^{-12}	"	"
1×10^{20}	75	"	1.6×10^{-6}	5.5×10^{-9}	6.2×10^{-20}	"	"
3×10^{20}	68	"	1.8×10^{-7}	3.5×10^{-9}	8.7×10^{-43}	"	"
1×10^{21}	60	"	2.4×10^{-9}	2.3×10^{-9}	—	"	"
3×10^{21}	52	"	9.2×10^{-10}	1.6×10^{-9}	—	"	8.0×10^{-3}
1×10^{22}	44	8.0×10^{-5}	3.9×10^{-10}	1.2×10^{-9}	—	"	5.0×10^{-3}

4. Temperature and density data. Computations were made for every 15° of latitude from 60° in the winter hemisphere to the summer pole and for heights from 45 to 115 km. Temperature and density data were mainly taken from COLE and KANTOR (1963) for the stratosphere and the mesosphere and from CHAMPION (1967) for the thermosphere. For the high latitude summer mesopause region a revision was considered desirable in accordance with recent temperature measurements. The temperatures and number densities used in the computations are listed in Tables 2—3 for intervals of 5 km.

5. Computation of number densities of oxygen-hydrogen components. In the computations in this section no transport processes were considered. The diurnal variation of solar radiation was, however, accounted for, although in a simplified way. Mean values for the dissociation rates were computed and taken as representative for daytime conditions. Daytime and nighttime number densities were then computed, taking into account the periodic interruption of solar radiation during the night. The term daytime number density of a component is here used to denote the concentra-

Table 2. *Upper air temperatures 45—115 km*

HEIGHT (KM)	LATITUDE							
	Summer				Winter			
	75°	60°	45°	30°	+15°	−30°	−45°	−60°
115	330.0	330.0	330.0	320.0	312.0	312.0	312.0	312.0
110	285.6	285.6	277.5	266.2	260.0	265.0	275.0	275.0
105	232.0	232.0	232.0	232.0	235.0	240.0	245.0	245.0
100	195.6	195.6	200.0	204.2	212.8	221.4	223.3	223.3
95	179.8	179.8	185.0	188.6	193.8	204.2	207.4	209.0
90	167.0	167.0	172.0	178.5	180.0	191.2	199.7	205.3
85	152.0	156.0	162.8	171.6	177.8	187.5	199.9	213.2
80	159.5	165.0	170.0	180.5	184.8	191.5	210.1	223.9
75	190.0	193.6	196.1	199.1	201.8	206.6	220.4	238.8
70	215.0	216.6	218.1	217.6	218.0	221.7	230.7	245.7
65	240.0	240.0	240.1	236.2	236.9	236.9	240.9	248.4
60	258.0	257.5	257.1	254,8	253.1	252.0	250.8	250.9
55	274.7	272.0	269.3	265.2	263.4	262.2	260.6	259.1
50	279.2	277.2	275.7	272.2	270.2	269.2	265.7	259.3
45	275.0	273.6	269.9	266.4	264.8	263.4	258.5	247.0

Table 3. *Number densities of air particles (45—115 km)*

HEIGHT (KM)	LATITUDE							
	Summer				Winter			
	75°	60°	45°	30°	+15°	−30°	−45°	−60°
115	8.25E+11	8.25E+11	8.50E+11	8.80E+11	9.15E+11	1.50E+12	1.52E+12	1.55E+12
110	1.60E+12	1.60E+12	1.68E+12	1.80E+12	1.93E+12	2.83E+12	2.96E+12	3.10E+12
105	3.65E+12	3.65E+12	4.00E+12	4.25E+12	4.60E+12	5.90E+12	6.20E+12	6.50E+12
100	9.44E+12	9.44E+12	9.79E+12	1.04E+13	1.10E+13	1.27E+13	1.35E+13	1.44E+13
95	2.60E+13	2.60E+13	2.70E+13	2.70E+13	2.80E+13	3.00E+13	3.15E+13	3.20E+13
90	7.21E+13	7.21E+13	7.18E+13	7.02E+13	7.02E+13	7.04E+13	7.19E+13	7.24E+13
85	2.02E+14	2.02E+14	1.97E+14	1.84E+14	1.79E+14	1.70E+14	1.65E+14	1.53E+14
80	5.29E+14	5.29E+14	5.05E+14	4.56E+14	4.34E+14	4.04E+14	3.54E+14	3.13E+14
75	1.17E+15	1.17E+15	1.11E+15	9.94E+14	9.41E+14	8.65E+14	7.32E+14	6.11E+14
70	2,37E+15	2.37E+15	2.23E+15	2.02E+15	1.92E+15	1.76E+15	1.47E+15	1.19E+15
65	4.58E+15	4.58E+15	4.20E+15	3.90E+15	3.70E+15	3.41E+15	2.85E+15	2.31E+15
60	7.93E+15	7.93E+15	7.60E+15	7.15E+15	6.84E+15	6.35E+15	5.42E+15	4.47E+15
55	1.42E+16	1.42E+16	1.37E+16	1.31E+16	1.26E+16	1.17E+16	1.01E+16	8.37E+15
50	2.58E+16	2.58E+16	2.50E+16	2.37E+16	2.29E+16	2.14E+16	1.86E+16	1.60E+16
45	4.81E+16	4.81E+16	4.72E+16	4.51E+16	4.37E+16	4.09E+16	3.62E+16	3.26E+16

tion at the end of the day (i.e. just before sunset), while the term nighttime number density here denotes the concentration at the end of the night (i.e. just before sunrise). Number densities computed in this way will be referred to as photochemical values.

For each level the total amounts of oxygen and hydrogen were assumed to be constant. All oxygen (in the forms of $O(^3P)$, $O(^1D)$, O_2, O_3, OH, HO_2, H_2O_2 and H_2O) counted as oxygen molecules, was assumed to be 20.95% of the total number density of air molecules. The choice of value for the mixing ratio of hydrogen is, as is well known, more uncertain. According to MASTENBROOK (1968), the average mixing ratio of water vapor at 20 km is likely to be 2.5×10^{-6}g/g. There is, however, reason to believe that molecular hydrogen and methane at 20 km together contribute an equal amount of hydrogen. The fractional content of hydrogen should then correspond to a water vapor mixing ratio of 5×10^{-6}g/g if all hydrogen at a given level were converted to water vapor.

On the basis of the reaction scheme listed in section 2, we may write down ten partial differential equations to express the time variations for the ten components in our model atmosphere. (In this report the number density of $O(^3P)$ will be denoted by $O(^3P)$ and similarly for the other components. The number density of air particles will be denoted by M.) For instance, the equation expressing the time variation of $O(^3P)$ may be written as

$$\frac{\partial O(^3P)}{\partial t} = -R_{O(^3P)} \cdot (O(^3P))^2 - Q_{O(^3P)} \cdot O(^3P) + P_{O(^3P)} \tag{5.1}$$

where $O(^3P)$ does not occur in the polynomials $P_{O(^3P)}$, $Q_{O(^3P)}$ and $R_{O(^3P)}$. Similarly we have for the other components

$$\frac{\partial O(^1D)}{\partial t} = -Q_{O(^1D)} \cdot O(^1D) + P_{O(^1D)} \tag{5.2}$$

$$\frac{\partial O_2}{\partial t} = -Q_{O_2} \cdot O_2 + P_{O_2} \tag{5.3}$$

$$\frac{\partial O_3}{\partial t} = -Q_{O_3} \cdot O_3 + P_{O_3} \tag{5.4}$$

$$\frac{\partial OH}{\partial t} = -R_{OH} \cdot (OH)^2 - Q_{OH} \cdot OH + P_{OH} \tag{5.5}$$

$$\frac{\partial HO_2}{\partial t} = -R_{HO_2} \cdot (HO_2)^2 - Q_{HO_2} \cdot HO_2 + P_{HO_2} \tag{5.6}$$

$$\frac{\partial H_2O_2}{\partial t} = -Q_{H_2O_2} \cdot H_2O_2 + P_{H_2O_2} \tag{5.7}$$

$$\frac{\partial H_2}{\partial t} = -Q_{H_2} \cdot H_2 + P_{H_2} \tag{5.8}$$

$$\frac{\partial H_2O}{\partial t} = -Q_{H_2O} \cdot H_2O + P_{H_2O} \tag{5.9}$$

$$\frac{\partial H}{\partial t} = -R_H \cdot H^2 - Q_H \cdot H + P_H \tag{5.10}$$

In addition we have the equations

$$(O(^1D) + O(^3P) + OH + H_2O)/2 + O_2 + HO_2 + H_2O_2 + 3 \cdot O_3/2 = \alpha M \quad (\alpha = 0.2095) \tag{5.11}$$

$$(OH + HO_2 + H)/2 + H_2O_2 + H_2 + H_2O = \beta M \quad (\beta = 8 \times 10^{-6}) \tag{5.12}$$

which may replace two of the partial differential equations in the numerical computations.

Fortunately these equations may be considerably reduced since most of the terms turn out to be relatively insignificant and may be neglected. These simplifications may change from level to level, and it is convenient to divide the atmosphere into regimes such that within each regime the same procedure may be used in the calculations. However, there are several simplifications which apply to a wide range of heights. In the first place the characteristic time for O(¹D) is always very short (less than one second). Photochemical equilibrium may then be assumed throughout for this component

$$O(^1D) = \frac{J_{2b} \cdot O_2 + J_{3b} \cdot O_3}{k_{20} \cdot M} \tag{5.13}$$

and substitution for $O(^1D)$ may be made in the other equations. The nighttime number density is extremely small and may be neglected in the computations. It may further be seen from Figure 4 that the number density of O(¹D) is negligible compared to the number density of O(³P). For the sake of brevity we shall use O, the total number density of atomic oxygen, for the number density of O(³P). From Figures 4 and 6 it follows that we may with a high degree of accuracy write

$$O_2 + O/2 = \alpha M \tag{5.14}$$

$$H/2 + H_2 + H_2O = \beta M \tag{5.15}$$

and these expressions will be used to make computations for the oxygen and hydrogen components having the highest number density.

Since we are dealing with altitudes from 45 km to 115 km it is, as already mentioned, convenient to divide this wide range into smaller regimes. It turns out to be convenient to treat separately the three regions 100—115 km, 70—100 km, and 45—70 km.

a. 100—115 km

This study does not aim at a detailed analysis of the composition of this part of the atmosphere but rather at pointing out the relative importance of the photochemical processes and obtaining a basis for the computation of dissociation rates below 100 km.

It is well known that the photochemical model atmosphere has failed to describe the distribution of molecular oxygen above 100 km. It was therefore decided to make use of observed values of the ratio O/O_2 (NIER et al., 1964, and SCHAEFER and NICHOLS, 1964). The values of O and O_2, computed in this way, were then used as constants in the expressions determining the number densities of ozone and the six hydrogen components. It can be seen from Figures 5 and 6 that practically all hydrogen is in atomic form ($H=2\beta M$).

The characteristic times for O and O_2 are very long and no diurnal variations will occur. The characteristic time for ozone is short (2 minutes for daytime and 4—16 minutes for nighttime conditions) and photochemical equilibrium is always a good approximation

$$O_3=\frac{k_2\cdot M\cdot O\cdot O_2}{J_3+k_3\cdot O+k_9\cdot H} \tag{5.16}$$

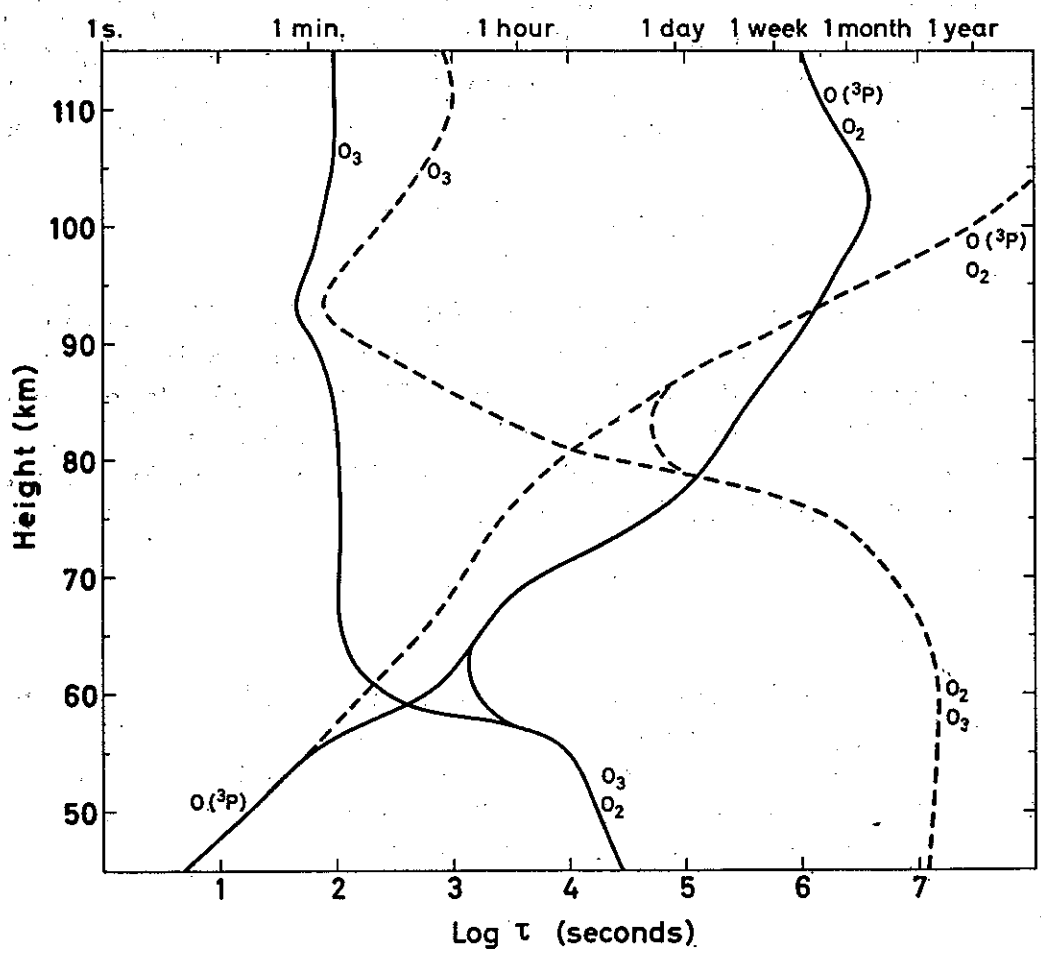

Fig. 1: Characteristic times for $O(^3P)$, O_2 and O_3 in a photochemical atmosphere model where transport processes are neglected. Solid curves refer to daytime conditions, dashed curves refer to nighttime conditions.

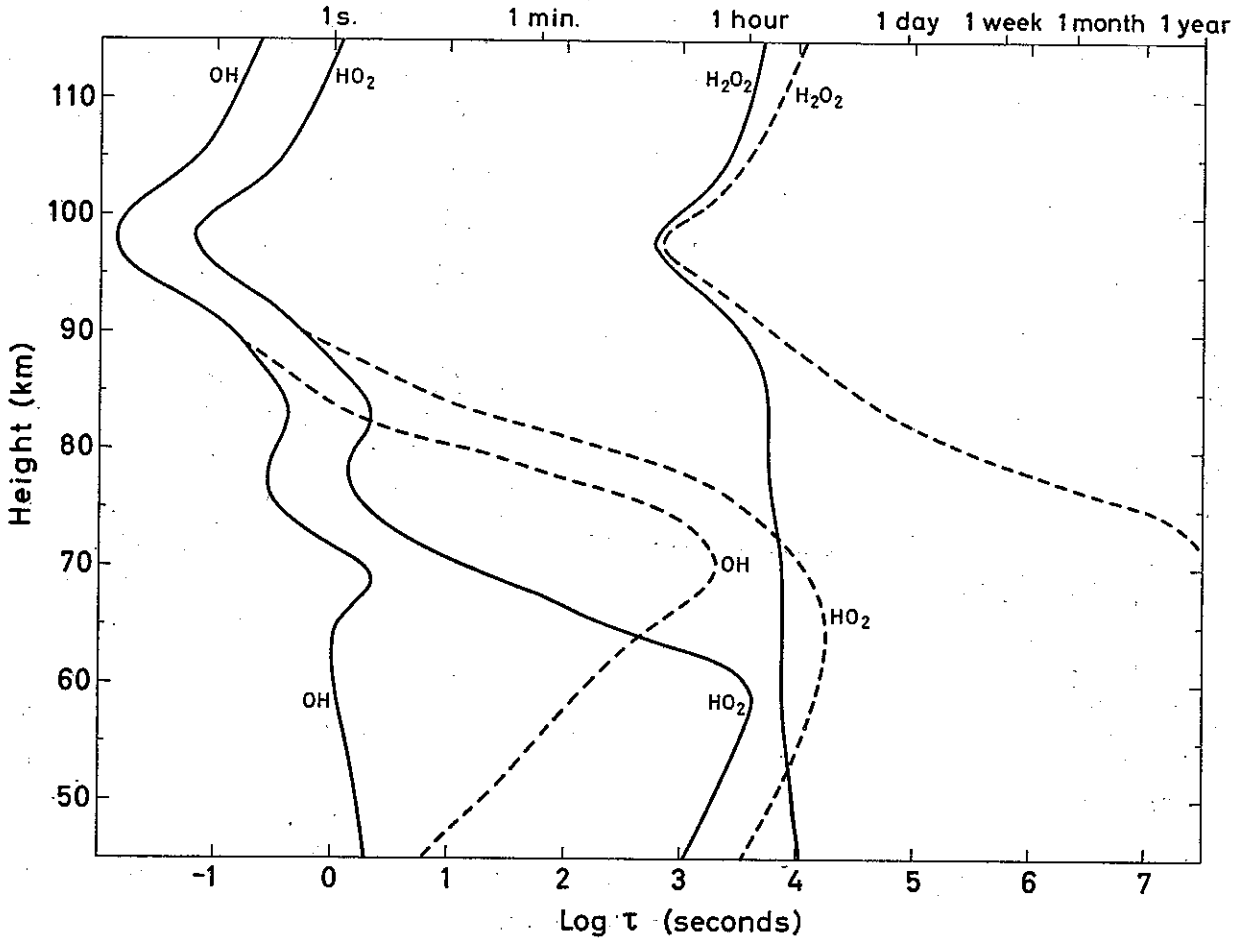

Fig. 2: Characteristic times for OH, HO_2 and H_2O_2 in a photochemical atmosphere model where transport processes are neglected. Solid curves refer to daytime conditions, dashed curves refer to nighttime conditions.

The characteristic times for OH and HO_2 are only fractions of a second. Photochemical equilibrium is rapidly established, and we obtain the following simplified expressions

$$HO_2=\frac{k_8\cdot M\cdot O_2\cdot H}{k_7\cdot O} \tag{5.17}$$

$$OH=\frac{k_7\cdot O\cdot HO_2+k_9\cdot O_3\cdot H}{k_6\cdot O}=\frac{k_8\cdot M\cdot O_2+k_9\cdot O_3}{k_6\cdot O}\cdot H \tag{5.18}$$

Above 100 km H_2O_2 is an extremely rare gas. The characteristic time is approximately 1/2—3 hours, i.e. less than a day. Photochemical equilibrium is then a fair approximation

$$H_2O_2=\frac{k_{13}\cdot(HO_2)^2}{J_{H_2O_2}+k_{12}\cdot O}=\frac{k_{13}\cdot(k_8\cdot M\cdot O_2\cdot H)^2}{(J_{H_2O_2}+k_{12}\cdot O)\cdot(k_7\cdot O)^2} \tag{5.19}$$

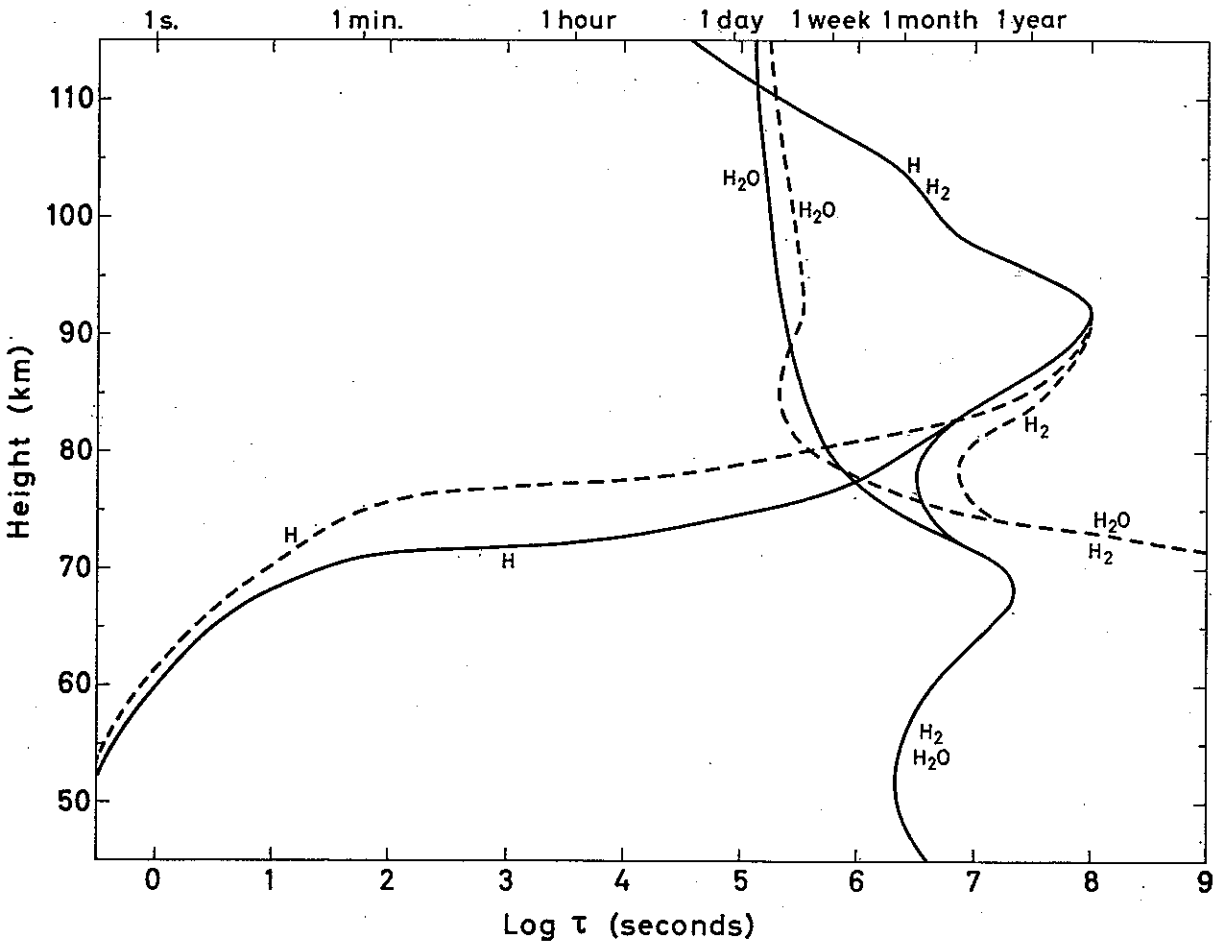

Fig. 3: Characteristic times for H, H_2 and H_2O in a photochemical atmosphere model where transport processes are neglected. Solid curves refer to daytime conditions, dashed curves refer to nighttime conditions.

We have not yet mentioned the components H_2 and H_2O. It will be shown later (section 6) that the photochemical values for these components are unrealistic above 70 km. Vertical eddy transport (below ~ 100 km) and molecular diffusion (above ~100 km) will transport H_2 and H_2O from below, and the photochemical values obtained from

$$H_2 \approx \frac{k_{18} \cdot HO_2 \cdot H + k_{19} \cdot M \cdot H^2}{k_{21} \cdot O(^1D) + k_{22} \cdot O} \tag{5.20}$$

$$H_2O \approx \frac{k_{17} \cdot H \cdot HO_2}{J_{H_2O}} \tag{5.21}$$

where substitutions may be made for HO_2, represent serious underestimates.

In section 6 we shall include vertical eddy transport between 65 km and 100 km in the computations. At the upper boundary we shall assume the photochemical values obtained in this subsection as boundary conditions at 100 km.

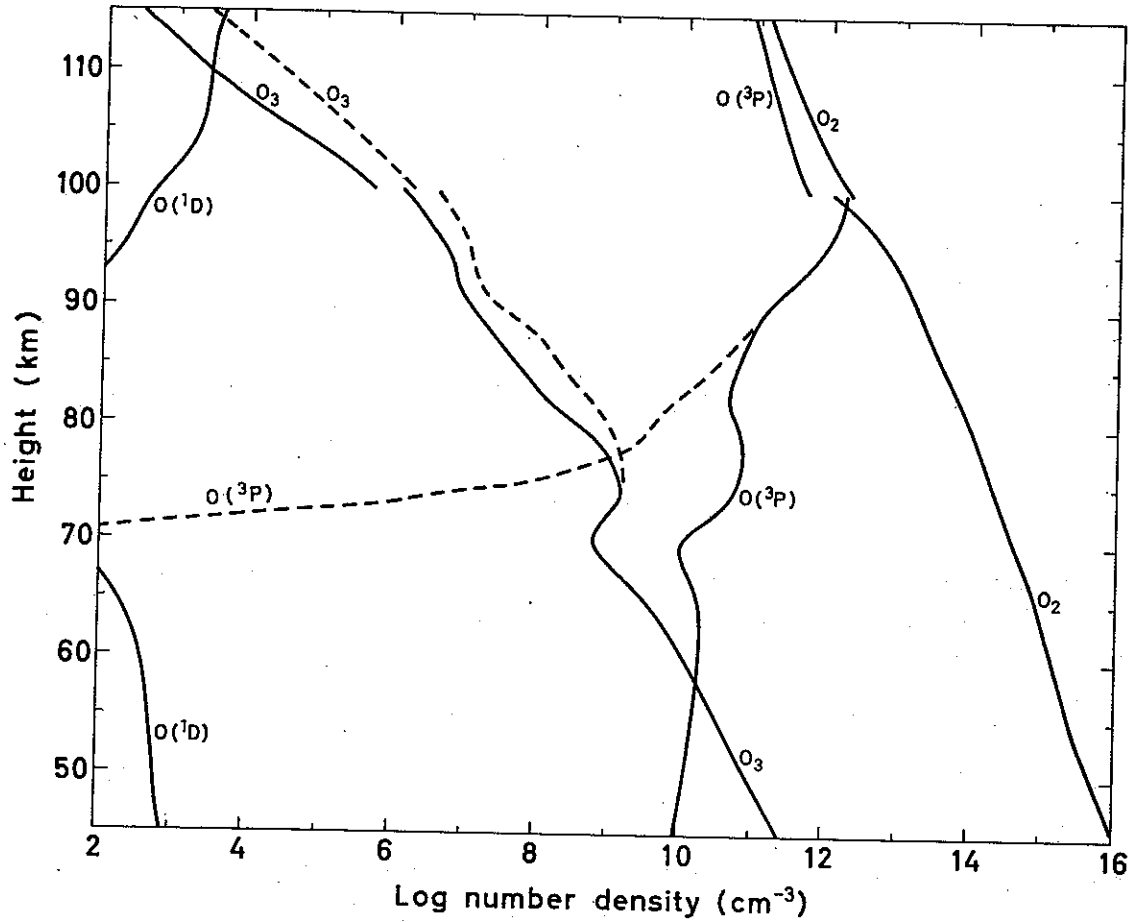

Fig. 4: Number densities of $O(^1D)$, $O(^3P)$, O_2 and O_3 in a photochemical atmosphere model where transport processes are neglected. Solid curves refer to daytime conditions, dashed curves refer to nighttime conditions.

b. 45—70 km.

In this part of the atmosphere photochemical equilibrium turns out to be a fairly realistic assumption for most of the components. Only H_2 and H_2O have characteristic times much longer than a day, and since H_2O takes up almost all the hydrogen in this region, H_2 is probably the only component for which the photochemical theory may give unrealistic results. Fortunately an error in the number density of H_2 does not influence the rest of the computations seriously.

A series of simplifications may be made in the complete expressions (5.1) to (5.10). As in the ozone layer, the terms $J_3 \cdot O_3$ and $k_2 \cdot M \cdot O \cdot O_2$ are the dominating terms in the expressions for $\partial O/\partial t$ and $\partial O_3/\partial t$. Since O is small in this region, the second order term in (5.1) may be neglected. A comparison between the terms $\tau_0^* = 1/Q_O$ and $\tau_{O_3}^* = 1/Q_{O_3}$ (which may be regarded as the first estimates of characteristic times) shows that the former is smaller below 58 km, while the latter is smaller above 59 km. Furthermore, the smaller of the two is always less than 2 minutes.

Considering first the region 59—70 km, we have with a sufficient degree of accuracy

$$O_3=\frac{k_2\cdot M\cdot O_d\cdot O_2}{J_3} \tag{5.22}$$

(when there is a diurnal variation of a component, index "d" is used to denote daytime number densities while index "n" is used for nighttime values). Since the characteristic time for ozone is very long for nighttime conditions no diurnal variations occur. If we assume $\partial O_3/\partial t=0$ and subtract (5.4) from (5.1), we obtain upon substitution of (5.22)

$$\frac{\partial O_d}{\partial t}=-\frac{2k_3\cdot k_2\cdot M\cdot O_2}{J_3}\cdot O_d^2-\left(k_6\cdot OH_d+k_7\cdot HO_{2,d}+\frac{k_9\cdot H_d\cdot k_2\cdot M\cdot O_2}{J_3}\right)\cdot O_d+2J_2\cdot O_2 \tag{5.23}$$

where a long series of unimportant terms have been neglected. From (5.23), where the second degree term is relatively small, we may compute the daytime equilibrium number density of atomic oxygen by setting $\partial O_d/\partial t=0$. Since the characteristic time is 1—2 hours, this value is nearly reached after noon.

The characteristic time of atomic oxygen during the night is less than half an hour. Photochemical equilibrium may therefore be assumed

$$O_n=\frac{k_{15}\cdot OH_n^2}{k_2\cdot M\cdot O_2} \tag{5.24}$$

Below 58 km the characteristic time is shorter for atomic oxygen than for ozone. Photochemical equilibrium may be assumed for daytime conditions

$$O_d=\frac{J_3\cdot O_3+2J_2\cdot O_2}{k_2\cdot M\cdot O_2+k_6\cdot OH_d+k_7\cdot HO_{2,d}} \tag{5.25}$$

as well as under nighttime conditions, when (5.24) is still valid.

The characteristic time for ozone increases from 4 hours at 58 km to 9 hours at 45 km for daytime conditions. Assuming $\partial O/\partial t=0$, subtracting (5.1) from (5.4), and neglecting insignificant terms, we obtain

$$\frac{\partial O_{3,d}}{\partial t}=-(2k_3\cdot O_d+k_9\cdot H_d+k_{23}\cdot HO_{2,d}+k_{24}\cdot OH_d)\cdot O_{3,d}+2J_2\cdot O_2 -(k_6\cdot OH_d+k_7\cdot HO_{2,d})\cdot O_d \tag{5.26}$$

which may be simplified because of the internal equilibrium in the $OH—HO_2—H$ cycle:

$$\frac{\partial O_{3,d}}{\partial t}=-2(k_3\cdot O_d+k_9\cdot H_d+k_{24}\cdot OH_d)\cdot O_{3,d}+2J_2\cdot O_2-2k_8\cdot M\cdot O_2\cdot H_d \tag{5.27}$$

where substitution for O_d may be made from (5.25). However, since the nighttime variation of ozone is negligible, and since transport processes are neglected, the number

density of ozone must be equal to its equilibrium value, which may be computed from (5.27) for $\partial O_{3,d}/\partial t=0$, i.e. from an ordinary second order equation in O_3.

Evidently $O_2=\alpha\cdot M$ throughout this region.

It has already been mentioned that OH, HO_2 and H form a reaction cycle. A possible departure from photochemical equilibrium between them is always restored in a few seconds time. Exchange of hydrogen between this group and other hydrogen components is, in general, a much slower process (characteristic times a few hours).

If we compare the quantities

$$\tau_{OH}^*=(Q_{OH}^2+4R_{OH}\cdot P_{OH})^{-\frac{1}{2}}\approx 1/Q_{OH},\quad \tau_{HO_2}^*=(Q_{HO_2}^2+4R_{HO_2}\cdot P_{HO_2})^{-\frac{1}{2}}$$

and

$$\tau_H^*=(Q_H^2+4R_H\cdot P_H)^{-\frac{1}{2}}\approx 1/Q_H,$$

it turns out that, under nighttime conditions, we have $\tau_H^*<\tau_{OH}^*<\tau_{HO_2}^*$ below 70 km. Since τ_H^* is shorter than 10 seconds, we may assume photochemical equilibrium for H:

$$H_n=\frac{k_{34}\cdot H_2\cdot OH_n}{k_8\cdot M\cdot O_2+k_9\cdot O_3} \tag{5.28}$$

where small terms have been neglected. τ_{OH}^* varies from 40 min. at 70 km to 2 min. at 60 km and 6 seconds at 45 km. Photochemical equilibrium is then a fair approximation (except in high latitudes, summer), and we may write

$$OH_n=\frac{k_{23}\cdot O_3\cdot HO_{2,n}}{k_{10}\cdot HO_{2,n}+k_{14}\cdot H_2O_2+k_{24}\cdot O_3}\approx\frac{k_{23}}{k_{24}}\cdot HO_{2,n} \tag{5.29}$$

Upon substitution for H_n and OH_n in the expression for $\partial HO_{2,n}/\partial t$ we obtain, when small terms are neglected,

$$\frac{\partial HO_{2,n}}{\partial t}=-2\left(\frac{k_{10}\cdot k_{23}}{k_{24}}+k_{13}\right)\cdot HO_{2,n}^2 \tag{5.30}$$

which may be integrated

$$HO_{2,n}=\frac{HO_{2,d}}{1+2\left(\frac{k_{10}\cdot k_{23}}{k_{24}}+k_{13}\right)\cdot HO_{2,d}\cdot t_n} \tag{5.31}$$

where t_n is the length of the night.

For daytime conditions we have $\tau_H^*<\tau_{OH}^*<\tau_{HO_2}^*$ below 60 km and $\tau_{OH}^*<\tau_H^*<\tau_{HO_2}^*$ between 60 and 70 km. Since the smallest of these quantities is always shorter than 10 seconds, photochemical equilibrium may be assumed for that component. Below 60 km we have

$$H_d=\frac{k_6\cdot OH_d\cdot O_d}{k_8\cdot M\cdot O_2+k_9\cdot O_3} \tag{5.32}$$

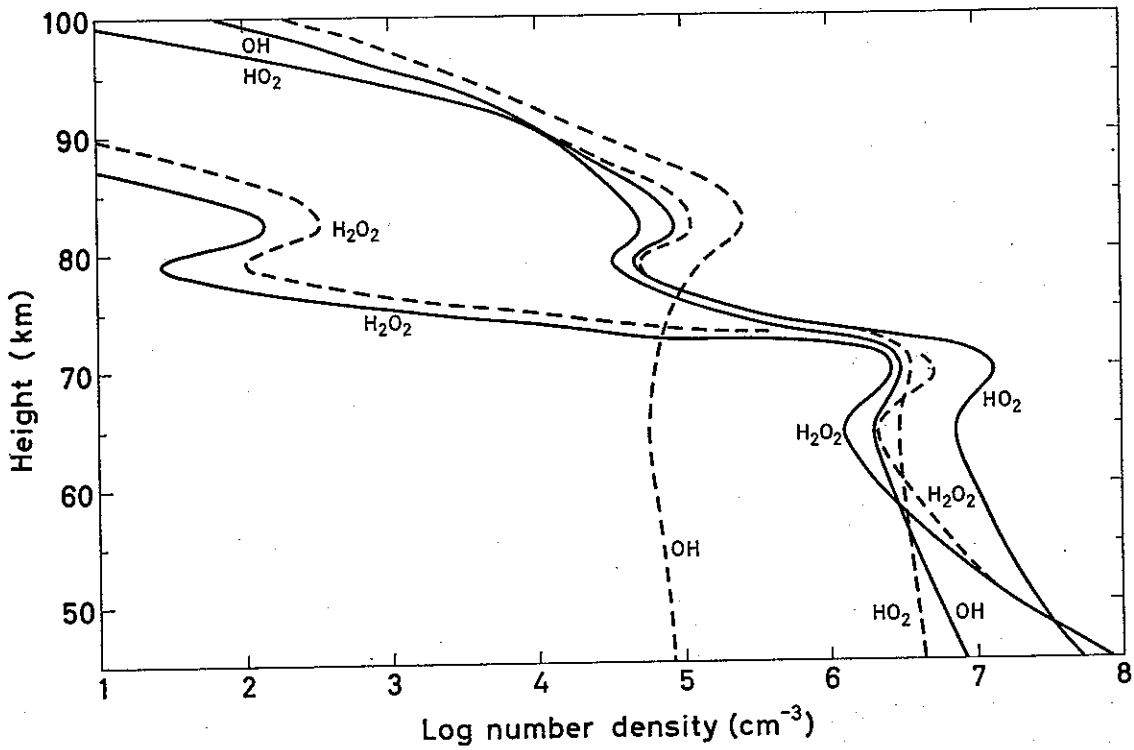

Fig. 5: Number densities of OH, HO_2 and H_2O_2 in a photochemical atmosphere model where transport processes are neglected. Solid curves refer to daytime conditions, dashed curves refer to nighttime conditions.

The characteristic time for OH is also very short, and photochemical equilibrium may be assumed

$$OH_d = HO_{2,d} \cdot \frac{k_7 \cdot O + k_{23} \cdot O_3}{k_6 \cdot O \cdot \gamma + k_{24} \cdot O_3} \approx HO_{2,d} \cdot \frac{k_7}{k_6 \cdot \gamma} \tag{5.33}$$

where

$$\gamma = \left(1 + \frac{k_8 \cdot O_3}{k_9 \cdot M \cdot O_2}\right)^{-1},$$

which is about 3/4 in our calculations. These expressions for H_d and OH_d are also valid up to 70 km. Substitution of (5.32) and (5.33) in the expression for $\partial HO_2/\partial t$ gives, when small terms are neglected,

$$\frac{\partial HO_{2,d}}{\partial t} = -R'_{HO_{2,d}} \cdot HO_{2,d}^2 + P'_{HO_{2,d}} \tag{5.34}$$

where

$$R'_{HO_{2,d}} = 2\left[\frac{k_{10} \cdot k_6}{\gamma k_7} + k_{13} + k_{15}\left(\frac{k_6}{\gamma k_7}\right)^2\right]$$

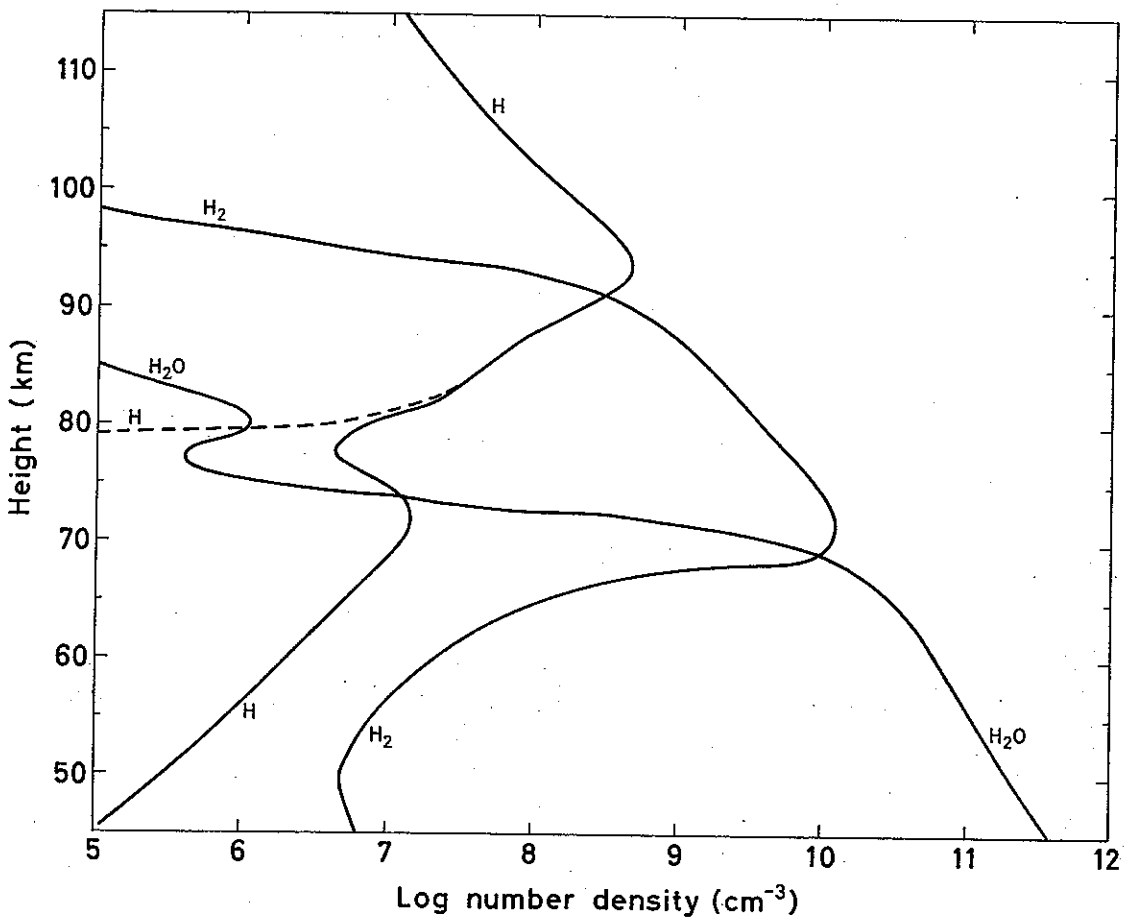

Fig. 6: Number densities of H, H_2 and H_2O in a photochemical atmosphere model where transport processes are neglected. Solid curves refer to daytime conditions, dashed curves refer to nighttime conditions.

$$P'_{HO_{2,d}}=2\{(J_{H_2O_2}+k_{12}\cdot O_d)\cdot H_2O_2+(J_{H_2O}+k_{29}\cdot O(^1D))\cdot H_2O+k_{21}\cdot O(^1D)\cdot H_2\} \tag{5.35}$$

The characteristic time is then

$$1/\sqrt{4R'_{HO_{2,d}}\cdot P'_{HO_{2,d}}}$$

and varies from 2 hours at 70 km to 40 min. at 45 km. Photochemical equilibrium is then a fairly good approximation even for $HO_{2,d}$:

$$HO_{2,d}=\sqrt{\frac{P'_{HO_{2,d}}}{R'_{HO_{2,d}}}} \tag{5.36}$$

H_2O_2 is a minor constituent in this region. It has a very long lifetime ($\sim$1 year) under nighttime conditions; under daytime conditions its lifetime is about 2—3 hours. With a sufficient degree of accuracy we may write

$$H_2O_2=\frac{k_{13}\cdot HO_{2,d}^2}{J_{H_2O_2}+k_{12}\cdot O_d+k_{14}\cdot OH_d}\approx\frac{k_{13}}{J_{H_2O_2}}\cdot HO_{2,d}^2 \tag{5.37}$$

Water vapor is the dominating hydrogen component below 70 km, and we may write

$$H_2O=\beta\cdot M-H_2 \tag{5.38}$$

where H_2 is negligible below 65 km. (It must however be borne in mind that the number density of molelcular hydrogen may be increased by turbulent downward transport from the source at 70—80 km).

Both H_2O and H_2 have very long lifetimes under nighttime conditions, and diurnal variations are negligible. The daytime variations are given by

$$\frac{\partial H_{2,d}}{\partial t}=-(k_{21}\cdot O(^1D)_d+k_{22}\cdot O_d+k_{34}\cdot OH_d)\cdot H_{2,d}+k_{18}\cdot H_d\cdot HO_{2,d}+k_{25}\cdot H_d\cdot H_2O_2 \tag{5.39}$$

$$\frac{\partial H_2O_d}{\partial t}=-\left(J_{H_2O}+\frac{k_{29}}{k_{20}}\cdot\frac{J_3\cdot O_3}{M}\right)\cdot H_2O_d+OH_d(k_{10}\cdot HO_{2,d}+k_{14}\cdot H_2O_2+k_{15}\cdot OH_d) \tag{5.40}$$

Since nighttime variations may be neglected, stationary conditions imply $\partial H_2O_d/\partial t=0$. Upon substitution of (5.39), (5.13), and (5.33), (5.40) then becomes an equation in OH_d. Stationary conditions also imply $\partial H_{2,d}/\partial t=0$, from which H_2 is computed.

Results of the computations are given in Figures 4, 5, and 6. Since so many of the parameters used are not well known, it would have been of great interest to compare the theoretical results with observational data. However, such data are only available for ozone, which is perhaps the most interesting component in this region. It was therefore decided to vary some of the parameters affecting ozone: β, k_2, k_3 and the ratio k_{29}/k_{20}. On the basis of rocket observations by JOHNSON, PURCELL, TOUSEY and WATANABE (1952), RAWCLIFFE, MELOY, FRIEDMAN, and ROGERS (1963), and by the Meteorological Office, England (private communication), we may define a reference profile

$$O_3=6\times10^{15-z/10} \tag{5.41}$$

where z is the height in km, which fits the observed profiles quite well. The reliability of our theoretical model atmosphere may then be tested by studying the ratio $\lambda=O_3/\tilde{O}_3$. A plot of λ is shown in Figure 7. It can be seen that for the values of the parameters used in the present paper, λ varies between about 1.6 in the lower part to about 2.2 in the upper part of the region 40—70 km (since it occurs for all choices of parameters, the decrease to lower values towards 70 km is probably caused by the reference profile rather than by the theoretical results). The deficiency of the present model atmosphere is seen to be eliminated if we make the following changes in the parameters

a) decrease k_2 by a factor of 2.5
or b) increase k_{29}/k_{20} by a factor of 10
or c) increase β by a factor of 5

These changes are within the range of uncertainties given.

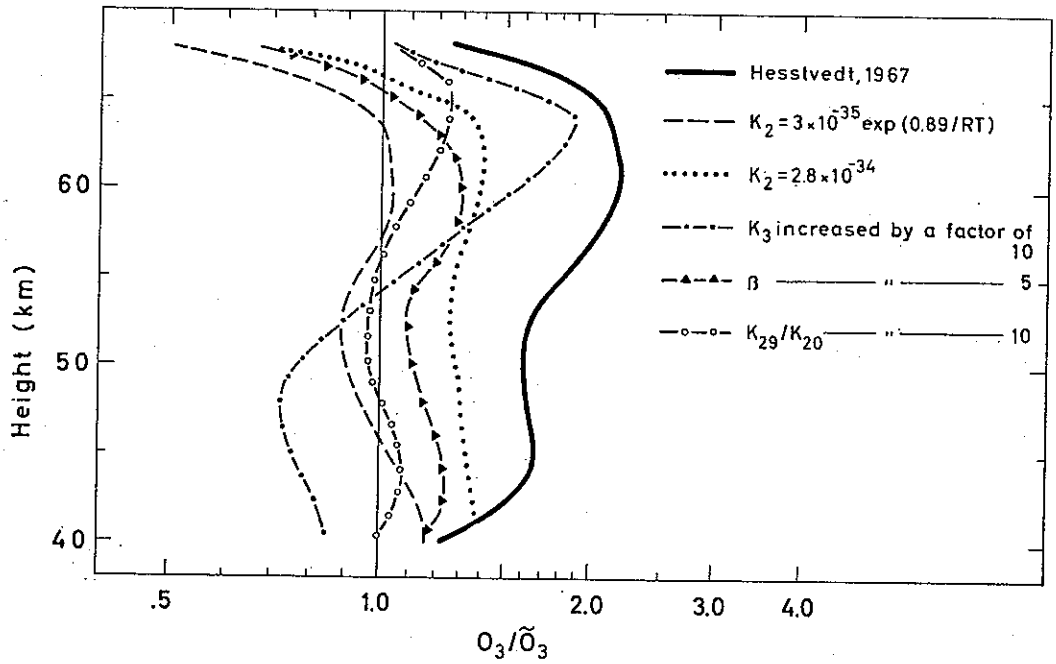

Fig. 7: Ratio between theoretical and observed values of the number density of ozone for different values of the most important parameters.

c. 70—100 km.

It has already been mentioned that transport processes are very important in this region, so that the photochemical model is quite unrealistic in many respects. Nevertheless a computation of photochemical values is most useful, since we learn a lot about the relative importance of the processes, about the characteristic times, and about the magnitude of diurnal variations.

In this region of 30 km depth the conditions undergo great changes from bottom to top, and it is inconvenient to use the same mathematical procedure for all levels. A marked change occurs at 80 km, where the characteristic time for atomic oxygen is of the order of a day.

For daytime conditions some of the components have very short characteristic times, and photochemical equilibrium may be assumed. Apart from (5.13) we have

$$O_{3,d} = \frac{k_2 \cdot M \cdot O_2 \cdot O_d}{J_3 + k_9 \cdot H_d} \tag{5.42}$$

$$HO_{2,d} = \frac{k_8 \cdot M \cdot O_2 \cdot H_d}{k_7 \cdot O_d} \tag{5.43}$$

$$OH_d = \frac{k_7 \cdot HO_{2,d} \cdot O_d + k_9 \cdot H_d \cdot O_{3,d}}{k_6 \cdot O_d} = \frac{M \cdot O_2}{k_6}\left(k_8 \cdot \frac{H_d}{O_d} + k_2 \cdot f_{O_s}\right) \tag{5.44}$$

where $f_{O_s} = k_9 \cdot H_d/(J_3 + k_9 \cdot H_d) < 1$.

For H_2O_2 the characteristic time is always less than two hours under daytime conditions. Photochemical equilibrium is then a fair assumption (especially since this component has very little influence upon the other nine components), and we may write

$$H_2O_{2,d}=\frac{k_{13}\cdot HO_{2,d}^2}{J_{H_2O_2}+k_{12}\cdot O_d+k_{14}\cdot OH_d+k_{25}\cdot H_d} \tag{5.45}$$

where substitution for OH_d and $HO_{2,d}$ may be made from (5.43) and (5.44).

The characteristic time for water vapor is long (3 days at 100 km, 4 days at 85 km, and more than 1 month below 75 km) both for daytime and nighttime conditions. The diurnal variations are therefore small and a mean value may be computed from

$$H_2O=\frac{P_{H_2O,d}+P_{H_2O,n}\cdot\frac{t_n}{t_d}}{J_{H_2O}} \tag{5.46}$$

where $t_d=$ length of the day, $t_n=$ length of the night and

$$P_{H_2O}=k_{10}\cdot OH\cdot HO_2+k_{15}\cdot OH^2+k_{17}\cdot H\cdot HO_2+k_{34}\cdot OH\cdot H_2 \tag{5.47}$$

where daytime and nighttime values should be inserted for use in (5.46). It should, however, again be mentioned that the number densities obtained from (5.46) are highly unrealistic. Vertical transport from below 70 km is fast enough to increase the water vapor content to orders of magnitude above the photochemical values.

H_2 has a long characteristic time ($\sim$1 month) throughout the whole region 70—100 km. Between 70 and 92 km H_2 is the most abundant hydrogen component, and its number density may be computed from (5.15). Above 92 km the time dependence is given by

$$\frac{\partial H_2}{\partial t}=-Q_{H_2}\cdot H_2+P_{H_2}=-[k_{21}\cdot O(^1D)+k_{22}\cdot O]\cdot H_2+[k_{18}\cdot f_{HO_2}+k_{19}\cdot M]\cdot H^2 \tag{5.48}$$

where $f_{HO_2}=HO_2/H$, given by (5.43). Since the diurnal variation is negligible, a mean value may be computed from

$$H_2=\frac{k_{18}\cdot H\cdot(HO_2\cdot t_d+HO_{2,n}\cdot t_n)+k_{19}\cdot M\cdot H^2\cdot(t_d+t_n)}{k_{21}\cdot O(^1D)\cdot t_d+k_{22}\cdot O\cdot(t_d+t_n)} \tag{5.49}$$

Above 92 km H is the dominating hydrogen component, and its number density in this region is computed from (5.15). In the region 70—92 km H may, in principle, be computed from the complete expression for $\partial H/\partial t$. This expression, however, is inconvenient for numerical computations, since the predominant terms in Q_H, $k_8\cdot M\cdot O_2+k_9\cdot O_3$, and in P_H, $k_6\cdot OH\cdot O$, have an algebraic sum which is very small. The daytime characteristic times of OH and HO_2 are shorter than that of H, although the difference becomes smaller and smaller as we descend towards 70 km. If we assume

photochemical equilibrium for OH and HO_2, we may, in the H-equation, substitute for the terms corresponding to reactions 6, 8, and 9. Neglecting small terms, (5.10) may then be written

$$\frac{\partial H}{\partial t} = -R'_H \cdot H^2 + P'_H \tag{5.50}$$

where

$$\begin{aligned} R'_H &= \left[2k_{10} \cdot f_{OH} \cdot f_{HO_2} + k_{15} \cdot f_{OH}^2 + (k_{17} + k_{18}) \cdot f_{HO_2} + k_{19} \cdot M + k_{25} \cdot \frac{H_2O_2}{H} \right] \\ P'_H &= [2J_{H_2O} \cdot H_2O + (k_{21} \cdot O(^1D) + k_{22} \cdot O) \cdot H_2] \end{aligned} \tag{5.51}$$

where $f_{OH} = OH/H$, given by (5.44). Since we have, in this region,

$$\beta M \approx H_2 + H/2, \quad \text{i.e.} \quad \frac{\partial H}{\partial t} + 2\frac{\partial H_2}{\partial t} \approx 0,$$

(5.51) corresponds very closely to (5.9). Upon substitution for H_2 from (5.15), (5.50) is suitable for integration, since the constant term and the coefficients for the first and second order terms are nearly constant during the time of integration (<24 hours).

Above 100 km atmospheric oxygen is, roughly speaking, evenly shared by O and O_2. As we descend below 100 km, O becomes gradually less important. O_2 is therefore most conveniently computed from (5.14) under daytime and nighttime conditions. Since O_3 has, in daytime, a much shorter characteristic time than O throughout this region, O_3 may, as well as OH, HO_2 and O_2, be substituted in (5.1), which then takes the form

$$\begin{aligned} \frac{\partial O_d}{\partial t} = &-[2k_1 - f_{O_3} \cdot k_2] \cdot M \cdot O_d^2 - [J_2 - k_8 \cdot M \cdot H_d + 2f_{O_3} \cdot k_2 \cdot \alpha \cdot M^2] \cdot O_d \\ &+ [2\alpha M \cdot (J_2 - k_8 \cdot M \cdot H_d)] \end{aligned} \tag{5.52}$$

As the terms in the brackets, with our definition of J_2, are nearly constant during the time of integration, (5.52) is suitable for a direct integration.

On the whole the integration of the equations (5.1) to (5.10) is relatively straightforward for daytime conditions. At night the conditions change considerably from 70 to 100 km, and the mathematical procedure may be different for different levels.

In the interval 80—100 km the characteristic time (night) of O is longer than that of O_3, and the characteristic time of H is longer than those of OH and HO_2. We then have

$$O_{3,n} = \frac{k_2 \cdot M \cdot O_2 \cdot O_n}{k_9 \cdot H_n} \tag{5.53}$$

$$HO_{2,n} = \frac{k_8 \cdot M \cdot O_2 \cdot H_n}{k_7 \cdot O_n} \tag{5.54}$$

$$OH_n=\frac{k_8\cdot M\cdot O_2+k_9\cdot O_{3,n}}{k_6\cdot O_n} \tag{5.55}$$

Substitution of $O_{3,n}$, OH_n, $HO_{2,n}$ and of $O_{2,n}=\alpha\cdot M-O_n/2$ results in (5.52) for $\mathcal{J}_2=\mathcal{J}_3=0$

$$\frac{\partial O_n}{\partial t}=-[(2k_1-k_2)\cdot M]O_n^2-[(2k_2\cdot\alpha\cdot M^2-k_8\cdot M\cdot H_n]\cdot O_n-[2\alpha\cdot M^2\cdot k_8H_n] \tag{5.56}$$

which may be integrated directly. O_d and O_n are then obtained from a combination of the integrated forms of (5.52) and (5.56).

The nighttime variation of H_2O_2 is not very important, since this component occurs in extremely small quantities. The nighttime equilibrium value

$$H_2O_{2,ne}=\frac{P_{H_2O_2,n}}{Q_{H_2O_2,n}}=\frac{k_{13}\cdot HO_{2,n}^2}{k_{12}\cdot O_n+k_{14}\cdot OH_n+k_{25}\cdot H_n} \tag{5.57}$$

is a good approximation above 90 km; between 70 and 90 km we may write

$$H_2O_{2,n}-H_2O_{2,ne}=(H_2O_{2,d}-H_2O_{2,ne})\cdot\exp(-t_n\cdot Q_{H_2O_2,n}) \tag{5.58}$$

For the three remaining components, H_2O, H_2 and H, the diurnal variations are small, and the values obtained above for daytime conditions are also representative of nighttime conditions above 80 km.

At about 80 km the characteristics of the atmospheric composition undergo a drastic change. Below this level atomic oxygen has a characteristic time shorter than a day, and since its equilibrium value for nighttime conditions is very small, large diurnal variations will take place. Because atomic oxygen is a very important agent in the reaction scheme, its variation has a great influence on the behavior of many of the other components. Atomic hydrogen also has a very short characteristic time during the nighttime, much shorter than OH and HO_2. Photochemical equilibrium is therefore a good approximation for H_n:

$$H_n=\frac{k_6\cdot OH_n+k_{22}\cdot H_2}{k_8\cdot M\cdot O_2+k_9\cdot O_{3,n}}\cdot O_n \tag{5.59}$$

If the equilibrium value of H_n is substituted in the expression for $\partial OH_n/\partial t$, it turns out that the characteristic time of OH_n is, in this region, always less than two hours. Photochemical equilibrium is then a fair approximation. Between 73 and 80 km we may write

$$OH_n=\frac{k_7\cdot O_n+k_{23}\cdot O_{3,n}}{\delta\cdot k_6\cdot O_n+k_{24}\cdot O_{3,n}}\cdot HO_{2,n} \tag{5.60}$$

where $\delta=(1-k_9\cdot O_{3,n}/k_8\cdot M\cdot O_2)^{-1}$. Below 73 km (5.29) may be used.

Nighttime variation of HO_2 is given by

$$\frac{\partial HO_{2,n}}{\partial t} = -2(k_{10} \cdot A + k_{13} + k_{15} \cdot A^2) \cdot HO_{2,n}^2 \tag{5.61}$$

(where the ratio $A = OH_n/HO_{2,n}$ may be taken from (5.60)), which may be integrated

$$HO_{2,n} = \frac{HO_{2,d}}{1 + 2(k_{10} \cdot A + k_{13} + k_{15} \cdot A^2) \cdot HO_{2,d} \cdot t_n} \tag{5.62}$$

O_2 is the dominating oxygen component and H_2 the dominating hydrogen component even for nighttime conditions, and their number densities may be computed from (5.14) and (5.15).

The nighttime concentrations of O and O_3 may be computed from the basic equations (5.1) and (5.4). When small terms are neglected, these equations may be approximated by

$$\frac{\partial O_n}{\partial t} = -(2k_2 \cdot M \cdot O_2 + k_6 \cdot OH_n + k_7 \cdot HO_{2,n}) \cdot O_n + k_{15} \cdot OH_n^2 \tag{5.63}$$

where the k_2-term is much larger than the k_6- and k_7-terms and the k_{15}-term is negligible above 72 km, and by

$$\frac{\partial O_{3,n}}{\partial t} = -(k_9 \cdot H_n + k_{23} \cdot HO_{2,n} + k_{24} \cdot OH_n) \cdot O_{3,n} + k_2 \cdot M \cdot O_2 \cdot O_n \approx k_2 \cdot M \cdot O_2 \cdot O_n \tag{5.64}$$

The terms in the brackets are negligible in comparison to the k_2-term down to 74 km. Below this level the diurnal variation is very small and may be neglected.

The computations were started on an IBM 1620 computer and continued on a CDC 3300. The set of equations was solved by an iterative method, using approximated analytical solutions to the differential equations as described above. In general the complete equations were used, but the substitutions, of course, introduce some errors, particularly in the regions where a shift from one procedure to another was necessary. However these errors were easy to detect and to smooth out. It is true that the height intervals given for the validity of specific assumptions may vary with latitude and season. They will also be influenced by the choice of parameters, in particular k_2. The calculations for 45°, summer, are shown in Figures 1, 2, and 3 for characteristic times and in Figures 4, 5, and 6 for number densities.

6. Oxygen-hydrogen atmosphere model with vertical eddy diffusion. Beyond any doubt the value of a purely photochemical atmosphere model must have its limitations. This has been demonstrated in a convincing way by the measurements of number densities of molecular oxygen above 100 km. For those levels the photochemical theory predicts very low values for O_2. However, O_2 is transported upwards by vertical diffusion, and when diffusion is included in the model, fair agreement is obtained between theory and observations.

As already mentioned (HESSTVEDT, 1964), vertical motion has a marked influence on the water vapor content near the mesopause. Since the horizontal number density gradients are relatively small, both horizontal mean motion and horizontal eddy diffusion will be of less importance than vertical mean motion and vertical eddy diffusion. Unfortunately, very little is known about the circulation in the mesosphere and thermosphere, and an introduction of a circulation in our atmosphere model will be more or less of academic interest. Even the vertical eddy diffusion coefficients are not well known. It will, however, be shown here that for a choice of diffusion coefficients within the range of possible values, several deficiencies of the static model are discarded. Modifications are primarily necessary for the distribution of O, H, H_2 and H_2O and consequently for other components, the number densities of which depend directly on these components.

As a step towards a more realistic oxygen-hydrogen model we shall include vertical eddy diffusion in our model atmosphere and make computations from 65 to 100 km for all latitudes, with the exception of the polar winter night. If the number density mixing ratio for a component is denoted by ρ, its variation due to diffusion may be calculated from

$$\left[\frac{\partial \rho}{\partial t}\right]_d = K_z \frac{\partial^2 \rho}{\partial z^2} + \frac{\partial K_z}{\partial z}\frac{\partial \rho}{\partial z} + \frac{K_z}{M}\frac{\partial M}{\partial z}\frac{\partial \rho}{\partial z} \tag{6.1}$$

The variation due to photochemistry alone may be written as

$$\left[\frac{\partial \rho}{\partial t}\right]_p = -R \cdot M \cdot \rho^2 - Q \cdot \rho + P/M \tag{6.2}$$

The total variation with time is then

$$\frac{\partial \rho}{\partial t} = -R \cdot M \cdot \rho^2 - Q \cdot \rho + P/M + K_z \frac{\partial^2 \rho}{\partial z^2} + \frac{\partial K_z}{\partial z}\frac{\partial \rho}{\partial z} + \frac{K_z}{M}\frac{\partial M}{\partial z}\frac{\partial \rho}{\partial z} \tag{6.3}$$

In the present model atmosphere we shall assume stationary conditions, i.e. $\partial \rho / \partial t = 0$. (6.3) may then be solved numerically by introducing finite differences for the derivatives

$$R \cdot M \cdot \rho^2 + Q \cdot \rho - P/M = \left[K_z \frac{\rho_a + \rho_b - 2\rho}{(\Delta z)^2} + \frac{(K_{za} - K_{zb})(\rho_a - \rho_b)}{(2\Delta z)^2} + \frac{K_z}{M}\frac{(M_a - M_b)(\rho_a - \rho_b)}{(2\Delta_z)^2} \right] \cdot M \tag{6.4}$$

where we shall take 1 km for the step Δz, and where the indices "a" and "b" refer to the points above and below the point for which the computation is made. (6.4) then becomes a second order (or, if $R = 0$, a first order) equation in ρ. The procedure will then be to start with a set of initial values, preferably the values obtained for the photochemical model, and scan over all levels until convergence is reached.

Our model extends from 65 to 100 km, and photochemical values for these levels were taken as boundary conditions. Computations have been made for $O(^3P)$, H, H_2 and H_2O. H_2 and H_2O have very long characteristic times and small diurnal variations between 65 km and 100 km and are allowed to diffuse between these two boundaries. The characteristic time of $O(^3P)$ becomes short at about 85 km, and diffusion is only considered between 85 km and 100 km. Similarly, the nighttime decrease of H is significant below 82 km, which is then taken as the lower boundary for diffusion of H. Below the lower boundaries photochemical values were assumed. $O(^1D)$, O_3, OH and HO_2 have short characteristic times, and photochemical values were assumed for these components. O_2 and H_2O_2 were computed in the usual way.

JOHNSON and WILKINS (1965) have computed upper limits for the vertical eddy diffusion coefficients. They used the heating rates given by MURGATROYD and GOODY (1958), and on the assumption of steady state in the temperature field they obtained values varying from 4×10^5 cm^2/s at 65 km to 7×10^6 cm^2/s at 100 km. These values are considerably lower than those obtained from sodium trail studies. For use in the present paper similar computations were made for different latitudes and for summer and winter. The eddy diffusion coefficients obtained are shown in Figure 8.

As in the purely photochemical model, the expressions for the source functions of the type (6.2) will vary from level to level, depending on the substitutions we are allowed to make at the level in question. Above 85 km the photochemistry is relatively simple, and for all practical purposes the following approximations may be made:

$$O(^1D)=\frac{J_{2b}\cdot O_2+J_{3b}\cdot O_3}{k_{20}\cdot M} \tag{6.5}$$

$$O_3=\frac{k_2\cdot M\cdot O_2\cdot O}{J_3+k_9\cdot H} \tag{6.6}$$

$$HO_2=\frac{k_8\cdot M\cdot O_2\cdot H}{k_7\cdot O} \tag{6.7}$$

$$OH=\frac{k_7\cdot HO_2\cdot O+k_9\cdot H\cdot O_3}{k_6\cdot O}=\frac{(k_8\cdot M\cdot O_2+k_9\cdot O_3)\cdot H}{k_6\cdot O} \tag{6.8}$$

$$H_2O_2=\frac{k_{13}\cdot(HO_2)^2}{J_{H_2O_2}+k_{12}\cdot O+k_{25}\cdot H} \tag{6.9}$$

These expressions are valid both for daytime and nighttime, and substitutions may be made in the expressions for the components having longer characteristic times:

$$\left(\frac{\partial O}{\partial t}\right)_p=-2k_1\cdot M\cdot O^2-\bar{f}_{O_3}\cdot k_2\cdot M\cdot O_2\cdot O+2\bar{J}_2\cdot O_2-2k_8\cdot M\cdot O_2\cdot H \tag{6.10}$$

$$\left(\frac{\partial H_2O}{\partial t}\right)_p = -\bar{J}_{H_2O} \cdot H_2O \tag{6.11}$$

$$\left(\frac{\partial H}{\partial t}\right) = 2\bar{J}_{H_2O} \cdot H_2O \tag{6.12}$$

$$\left(\frac{\partial H_2}{\partial t}\right)_p = -[k_{21} \cdot O(^1D) + k_{22} \cdot O(^3P)] \cdot H_2 + k_{18} \cdot H \cdot HO_2 + k_{19} \cdot M \cdot H^2$$

$$= -[k_{21} \cdot O(^1D) + k_{22} \cdot O] \cdot H_2 + \left[\frac{k_{18} \cdot k_8 \cdot O_2}{k_7 \cdot O} + k_{19}\right] \cdot M \cdot H^2 \tag{6.13}$$

where $f_{O_3} = (1 + J_3/k_9 \cdot H)^{-1}$ and bars denote daily mean values.

These four expressions (6.10 to 6.13) are then combined with equation (6.4) and solved by iterations as indicated above.

Below 85 km the characteristic time for $O(^3P)$ becomes so short that diurnal variation is considerable. 85 km was therefore taken as the lower boundary for diffusion of $O(^3P)$. For a similar reason 82 km was taken as the lower boundary for diffusion of H. H_2 and H_2O still have long characteristic times down to 65 km, the lower boundary of our model. The photochemistry for these components in the region 65 to 85 km is given by

$$\left(\frac{\partial H_2O}{\partial t}\right)_p = -(J_{H_2O} + k_{29} \cdot O(^1D)] \cdot H_2O + [k_{10} \cdot HO_2 \cdot OH + k_{14} \cdot OH \cdot H_2O_2 + k_{17} \cdot H \cdot HO_2] \tag{6.14}$$

and by

$$\left(\frac{\partial H_2}{\partial t}\right)_p = -[k_{21} \cdot O(^1D) + k_{22} \cdot O(^3P) + k_{34} \cdot OH] \cdot H_2 + [(k_{18} \cdot HO_2 + k_{25} \cdot H_2O_2) \cdot H] \tag{6.15}$$

where the first degree term in H_2 is unimportant down to 70 km. Daily mean values should be used for the expressions in brackets in (6.14) and (6.15). The number densities of the rest of the components are obtained as in the photochemical model. It should be noted, however, that the increase in water vapor due to diffusion causes some important changes in the relative importance of the reactions. As always, the number density of $O(^1D)$ is given by (6.5), while O_2 may be taken as constant and equal to αM. The number density of atomic oxygen is given by

$$\frac{\partial O}{\partial t} = -[2k_1 \cdot M \cdot O + f_{O_3} \cdot k_2 \cdot M \cdot O_2 + k_6 \cdot OH + k_7 \cdot HO_2] \cdot O + 2J_2 \cdot O_2 \tag{6.16}$$

for daytime conditions and by

$$\frac{\partial O_n}{\partial t} = -[k_2 \cdot M \cdot O_2 + k_6 \cdot OH_n + k_7 \cdot HO_{2,n}] \cdot O_n + k_{15}(OH_n)^2 \tag{6.17}$$

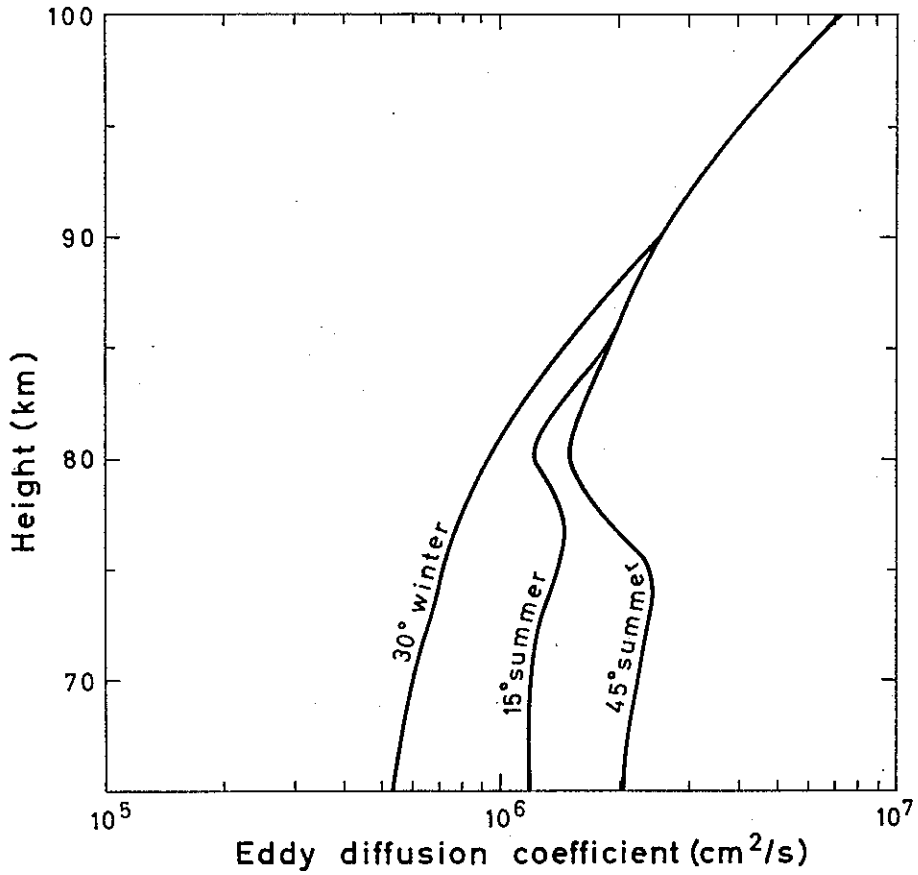

Fig. 8: Vertical eddy diffusion coefficients used in the present calculations.

for nighttime conditions. For daytime conditions photochemical equilibrium may be assumed below 83 km

$$O=\frac{2J_2\cdot O_2}{f_{O_3}\cdot k_2\cdot M\cdot O_2+k_6\cdot OH+k_7\cdot HO_2} \tag{6.18}$$

where the k_2-term is smaller than the k_6- and k_7-terms, and for nighttime below 74 km we have

$$O_n=\frac{k_{15}\cdot(OH_n)^2}{k_2\cdot M\cdot O_2+k_6\cdot OH_n+k_7\cdot HO_{2,n}} \tag{6.19}$$

where the k_2-term is the largest term in the denominator.

Ozone is in photochemical equilibrium down to 65 km during the day, and its number density is given by

$$O_3=\frac{k_2\cdot M\cdot O_2\cdot O}{J_3+k_9\cdot H} \tag{6.20}$$

During the night we have

$$\frac{\partial O_{3,n}}{\partial t}=-[k_9\cdot H_n+k_{23}\cdot HO_{2,n}+k_{24}\cdot OH_n]\cdot O_{3,n}+k_2\cdot M\cdot O_2\cdot O_n \tag{6.21}$$

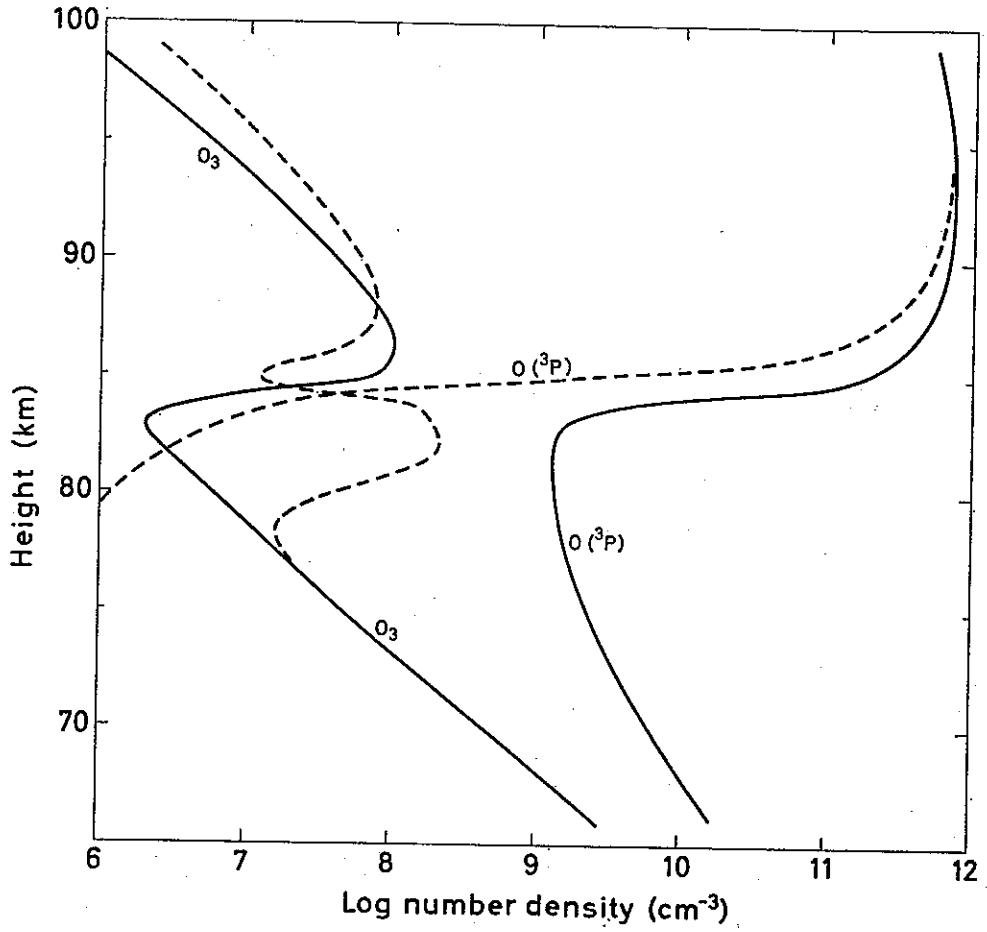

Fig. 9: Number densities of O and O_3 in a photochemical atmosphere model with vertical eddy diffusion. Solid curves refer to daytime conditions, dashed curves refer to nighttime conditions.

and since the characteristic time is relatively long and increases downward, photochemical equilibrium is never reached. Below 75 km the nighttime variation of ozone is very small and may be neglected.

For OH and HO_2 we may assume photochemical equilibrium during the day, and when small terms are neglected we may write

$$HO_2 = \frac{k_8 \cdot M \cdot O_2 \cdot H}{k_7 \cdot O + k_{30} \cdot H} \tag{6.22}$$

where the k_7-term is the largest term in the denominator, and

$$OH = \frac{k_7 \cdot O \cdot HO_2 + k_9 \cdot O_3 \cdot H + 2k_{30} \cdot H \cdot HO_2}{k_6 \cdot O}$$

$$= \frac{(k_8 \cdot M \cdot O_2 + k_9 \cdot O_3 + k_{30} \cdot HO_2) \cdot H}{k_6 \cdot O} \tag{6.23}$$

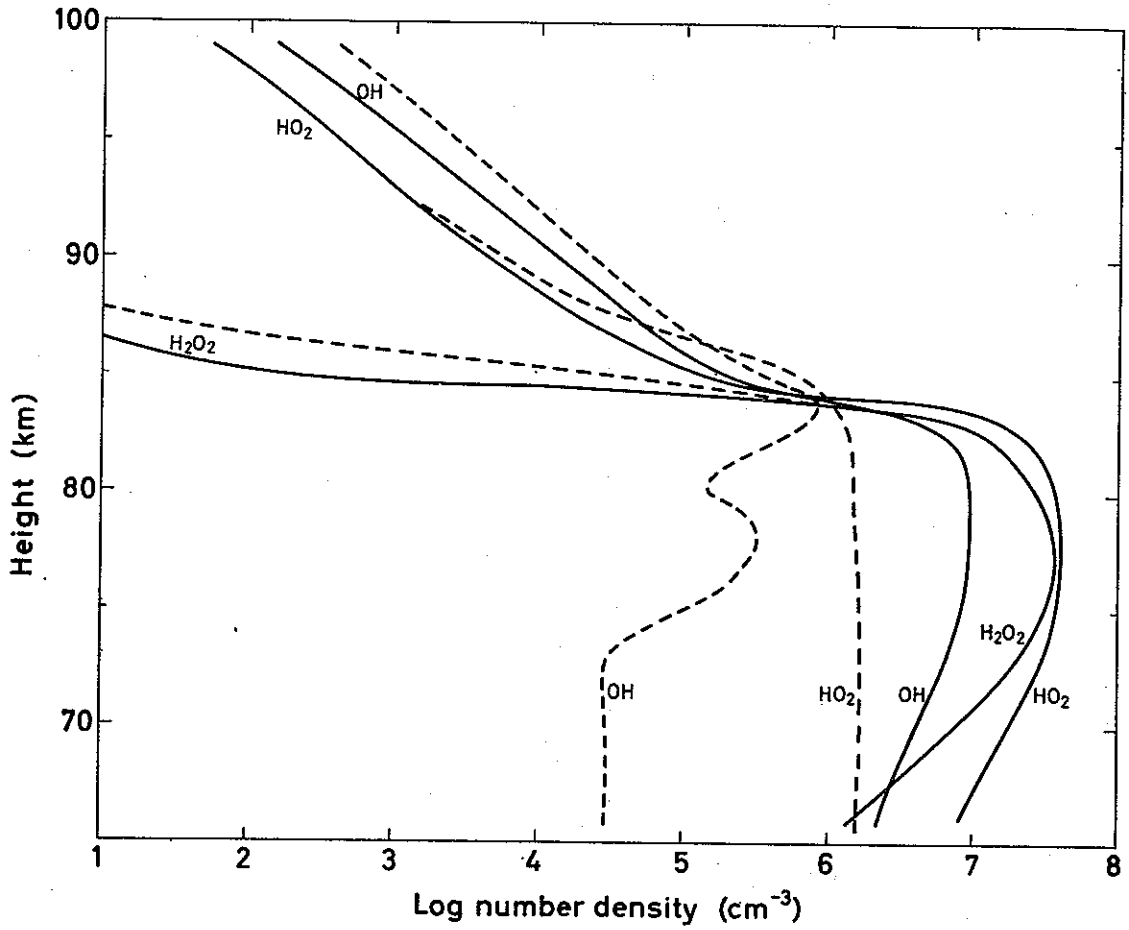

Fig. 10: Number densities of OH, HO_2 and H_2O_2 in a photochemical atmosphere model with vertical eddy diffusion. Solid curves refer to daytime conditions, dashed curves refer to nighttime conditions.

where the k_8-term is the largest term in the numerator. With a sufficient degree of accuracy we may assume that H_2O_2 is also in photochemical equilibrium during the day

$$H_2O_2 = \frac{k_{13} \cdot (HO_2)^2}{J_{H_2O_2} + k_{12} \cdot O + k_{14} \cdot OH + k_{25} \cdot H} \tag{6.24}$$

Since OH and HO_2 have very short characteristic times during the day, substitutions may be made in the expression for $\partial H/\partial t$. And since the characteristic time for H also turns out to be relatively short, photochemical equilibrium is a very good approximation below 83 km:

$$H = \sqrt{\frac{J_{H_2O_2} \cdot H_2O_2 + J_{H_2O} \cdot H_2O}{k_{10} \cdot \frac{OH}{H} \cdot \frac{HO_2}{H} + k_{13}\left(\frac{HO_2}{H}\right)^2 + k_{15}\left(\frac{OH}{H}\right)^2 + k_{18}\frac{HO_2}{H}}} \tag{6.25}$$

where the ratios in the denominator are obtained from (6.22) and (6.23)

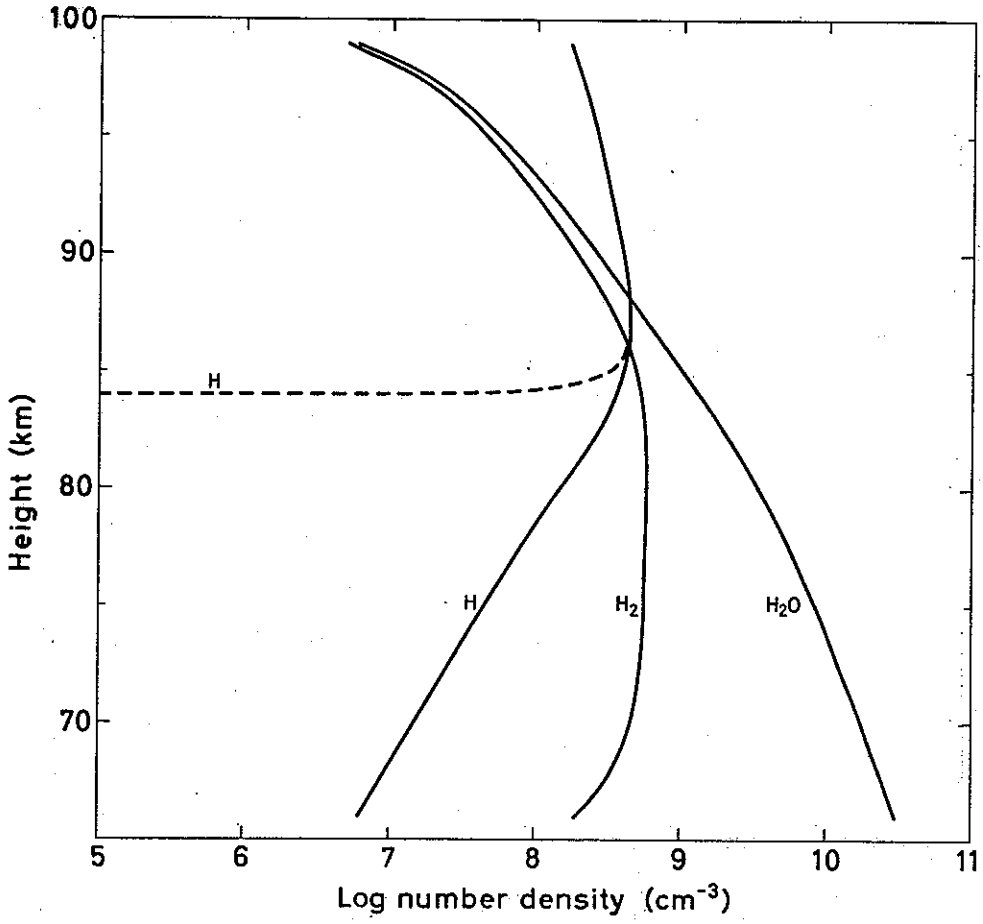

Fig. 11: Number densities of H, H_2 and H_2O in a photochemical atmosphere model with vertical eddy diffusion. Solid curves refer to daytime conditions, dashed curves refer to nighttime conditions.

As in the photochemical model, the number density of OH changes considerably from day to night. Below 73 km we may write

$$OH_n = \frac{k_{23} \cdot O_{3,n} \cdot HO_{2,n}}{k_{24} \cdot O_{3,n} + k_{10} \cdot HO_{2,n} + k_{14} \cdot H_2O_{2,n}} \tag{6.26}$$

Between 74 and 85 km the characteristic time is of the order of hours and photochemical equilibrium is almost, but not quite, reached. The nighttime variation is given by

$$\frac{\partial OH_n}{\partial t} = -[k_6 \cdot O_n + k_{10} \cdot HO_{2,n} + k_{14} \cdot H_2O_{2,n} + k_{24} \cdot O_{3,n}] \cdot OH_n$$
$$+[k_7 \cdot O_n \cdot HO_{2,n} + k_9 \cdot O_{3,n} \cdot H_n + k_{23} \cdot O_{3,n} \cdot HO_{2,n}] \tag{6.27}$$

The nighttime variation of atomic hydrogen is approximately given by

$$\frac{\partial H_n}{\partial t} = -[k_8 \cdot M \cdot O_2 + k_9 \cdot O_{3,n}] \cdot H_n + [k_6 \cdot O_n + k_{34} \cdot H_2] \cdot OH_n \tag{6.28}$$

Below 83 km photochemical equilibrium is a good approximation

$$H_n = \frac{k_6 \cdot O_n + k_{34} \cdot H_2}{k_8 \cdot M \cdot O_2 + k_9 \cdot O_{3,n}} \cdot OH_n \tag{6.29}$$

Since OH and H have very short characteristic times below 73 km, substitutions may be made in the expression for $\partial HO_{2,n}/\partial t$ to give

$$\frac{\partial HO_{2,n}}{\partial t} = -2\left[k_{10} \cdot \frac{k_{23}}{k_{24}} + k_{13} + k_{15}\left(\frac{k_{23}}{k_{24}}\right)^2\right] \cdot HO_{2,n}^2 \approx -2k_{13} \cdot HO_{2,n}^2 \tag{6.30}$$

which may be integrated

$$HO_{2,n} \approx \frac{HO_{2,d}}{1 + 2k_{13} \cdot HO_{2,d} \cdot t_n} \tag{6.31}$$

Above 73 km OH is not quite in equilibrium and the nighttime variation in HO_2 is given by

$$\frac{\partial HO_{2,n}}{\partial t} = -2k_{13} \cdot HO_{2,n}^2 - [k_7 \cdot O_n + k_{10} \cdot OH_n + k_{23} \cdot O_{3,n}] \cdot HO_{2,n}$$
$$+ [f_1 \cdot k_6 \cdot O_n + k_{14} \cdot H_2O_{2,n} + k_{24} \cdot O_{3,n}] \cdot OH_n \tag{6.32}$$

where $f_1 = [(1 + k_9 \cdot O_{3,n}/(k_8 \cdot M \cdot O_2)]^{-1}$. f_1 varies from about 0.2 to 85 km to about 0.9 at 72 km.

The results of the computations are shown in Figures 9—11. A comparison with the results from the photochemical model, given in Figures 4—6, shows that the most striking change lies in the mixing ratios of the major hydrogen components, H, H_2 and H_2O. When eddy transport is neglected, the model gives very low number densities for water vapor above 72 km. But in view of the long characteristic time for water vapor (1—7 days), it is quite clear that vertical eddy transport must have a drastic influence on the vertical distribution. In the present calculation water vapor takes up 85% of all available hydrogen at 80 km; the corresponding figure is 60% at 85 km, 40% at 90 km, and 25% at 95 km. This is a very important point in the discussion of the nature of noctilucent clouds. It has been suggested that such clouds consist of ice particles. Such a viewpoint may be supported by the present calculations, whereas older models, where vertical eddy diffusion was neglected, exclude the possibility of ice particle growth.

The purely photochemical model predicted an H_2-regime between 70 and 90 km. It is seen from Figure 11 that this regime is almost broken down. The lower mesosphere, with its low number densities of H_2, acts as an effective sink with a noticeable effect up to 90 km.

Eddy diffusion may also be seen (from Figures 4 and 9) to have an important effect on the distribution of atomic oxygen and consequently on ozone. Atomic oxygen is effectively transported downward to the mesopause, where the characteristic time becomes so short that the nocturnal breakdown represents an effective barrier for further transport. The marked peak of atomic oxygen at 100 km, as found in the purely photo-

chemcial model, is transformed to a broad maximum centered around 90—95 km. The change in the atomic oxygen profile has an important bearing on theoretical computations of airglow. This will be considered in section 7.

The simplifications and the mathematical procedures described in this section are valid for computations for 45° latitude, summer. Small alterations are necessary when computations are made for other latitudes and seasons.

One important result of the present model is that horizontal gradients in the number densities are relatively small, as long as we exclude the results for the regions adjacent to the polar winter night area. This means that horizontal transport, by eddies or by mean motion, are in general of less importance. On the other hand vertical mean motion may have an influence. This is especially true in polar regions, since vertical velocities are believed to be small in low and middle latitudes.

It has been suggested (KELLOGG, 1961, YOUNG and EPSTEIN, 1962, HESSTVEDT, 1965) that recombination of atomic oxygen may be an important heat source in the lower thermosphere, and that this heating should be especially important in high latitudes during the winter. This heating may be calculated from

$$\frac{\Delta T}{\Delta t}=\frac{E_1 \cdot k_1 \cdot M \cdot O^2}{c_p \cdot \rho}=4\left(\frac{O}{10^{12}}\right)^2 {}^0K/\text{day} \tag{6.33}$$

where $E_1=5.1$ eV is the energy released in reaction (1). In the present model this heating will amount to maximum 2°K/day. An increase may be expected when we have a downward motion. A vertical velocity of 1 cm/s (downward) will hardly effect the heating rate. If the vertical velocity is increased to 5 cm/s, the maximum heating rate will be about 4°K/day. These figures, however, should be regarded as tentative. Relatively small variations in the parameters may result in considerable variations in the heating rates. But it is very unlikely that "realistic" values of the parameters will lead to such high heating rates as have been obtained in previous models.

The big difference between the present and the previous results is mainly due to two differences in the basic assumptions.

a) in the present model lower densities have been used. Consequently the number density of atomic oxygen, which occurs squared in (6.33), is lower in the present model

b) in previous models a pure oxygen atmosphere model was used. The introduction of hydrogen will reduce the number density of atomic oxygen and give lower heating rates.

7. Airglow. On the basis of the number densities computed above, we may evaluate theoretical values for the intensities of the OH* emission and the atomic oxygen green line emission. Considering first the OH* emission, two mechanisms have been considered as responsible for the excitation of the OH molecule: the ozone-hydrogen process, proposed by BATES and NICOLET (1950)

$$O_3+H\rightarrow OH^*+O_2 \tag{7.1}$$

and the KRASSOVSKIJ process

$$O_2^*+H\rightarrow OH^*+O \tag{7.2}$$

Since the first reaction is identical with reaction 9 in our scheme, the resulting nightglow intensity from a point is given by

$$E_{BN}=4k_9\cdot O_{3,n}\cdot H_n \tag{7.3}$$

since, on the average, each excitation is believed to result in an emission of four photons. Computations show that the contribution to the total emission from levels above 100 km and below 83 km is small and may be neglected. Above 85 km the characteristic time for ozone is only a few minutes during the night and photochemical equilibrium may be regarded as a good approximation

$$E_{BN}=4k_9\cdot H_n\cdot\frac{k_2\cdot M\cdot O_2\cdot O_n}{k_3\cdot O_n+k_9\cdot H_n}\approx 4k_2\cdot M\cdot O_2\cdot O_n \tag{7.4}$$

since $k_3O_n\ll k_9\cdot H_n$. This means that the result of the computation does not depend directly upon the value adopted for β, defined by (5.12). But there is, of course, an indirect relationship, since the number density of atomic oxygen depends on β because of the reactions with OH and HO_2.

In computing the frequency of the KRASSOVSKIJ-process we run into difficulties, because the reactions determining the deexcitation of excited oxygen molecules are not well known. Without further discussion we shall assume that O_2* is always in photochemical equilibrium (its lifetime is necessarily very short), given by

$$k_1\cdot M\cdot O_n^2=(A+k'\cdot O_n)\cdot O_2^* \tag{7.5}$$

where we assume $A=0.18$ and $k'=10^{-13}$ cm^3/s (reference is made to YOUNG and EPSTEIN, 1962). The contribution from process (7.2) to the OH* emission will then be

$$E_K=4k''\cdot k_1\cdot M\cdot O_n^2\cdot H_n/(A+k'\cdot O_n) \tag{7.6}$$

where we shall assume $k''=10^{-10}$ cm^3/s. Using the nighttime number densities of O and H as computed above, we find that process (7.2) will only contribute by about 1% of the total OH* emission. This supports the viewpoint that process (7.1) is the dominating excitation mechanism below 105 km, i.e. throughout the region where the OH* emission is intense. However, if the value of k'' is much higher than 10^{-10} cm^3/s, or if the hydrogen content is much higher than assumed here, our conclusion about the importance of process (7.2) may be questionable.

The results of the computations are given in Figure 12. It can be seen that the model predicts only small variations according to latitude and season, in good agreement with observations. (It must, however, be emphasized here that the different curves in Figure 12 are *not* meant to indicate the trend of a possible variation according to latitude and season. The uncertainty in the determination of the diffusion coefficients is too large for such a conclusion. The curves only indicate that no large variations are likely to occur in regions with small vertical velocities.) With regard to the level of maximum emission, good agreement has been obtained with the rocket experiments of HEPPNER

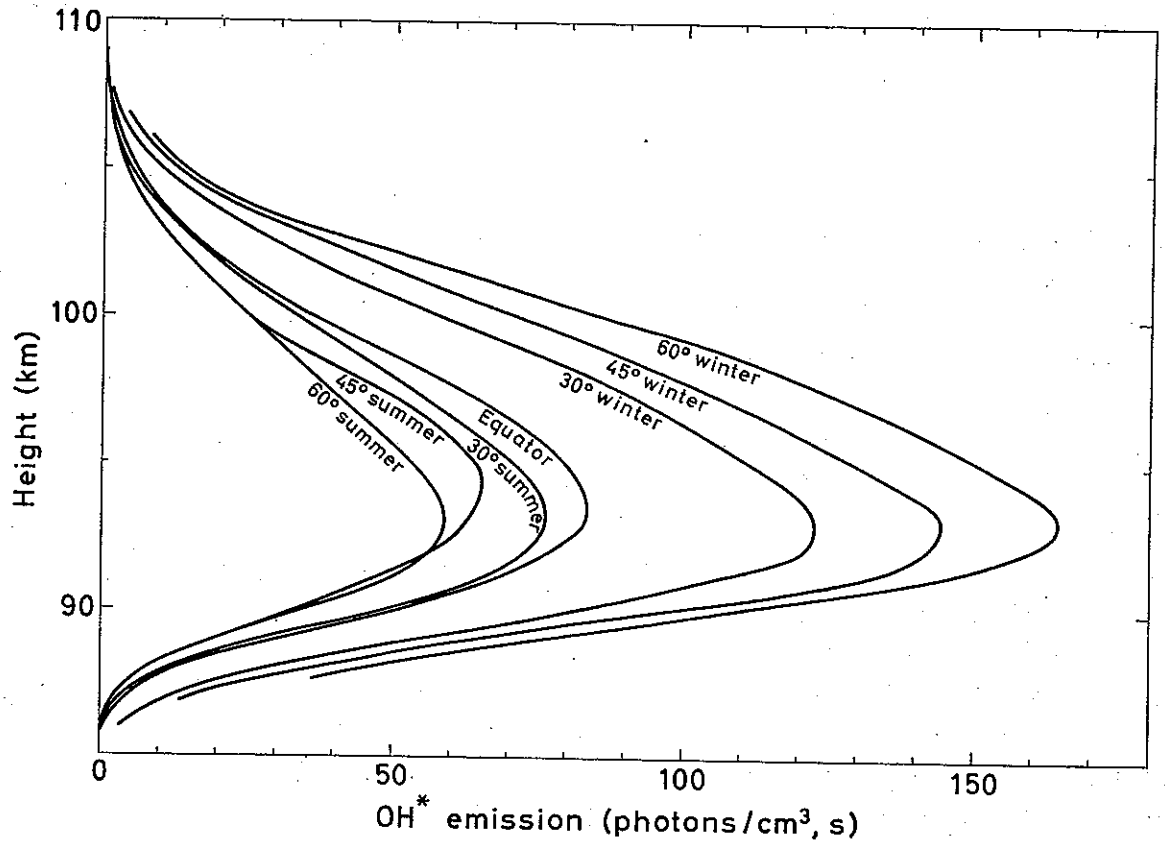

Fig. 12: Theoretical profiles for OH*-emission in the nightglow in a photochemical model atmosphere with vertical eddy diffusion.

and MEREDITH (1958), LOWE (1960), PACKER (1961), and TARASOVA (1961). On the other hand our model is not capable of explaining a recent measurement by BAKER (1967) who found an emission peak at 98 km.

The global mean value of the OH* emission is assumed to be about 4800 kR CHAMBERLAIN and SMITH, 1959). Here a theoretical mean value of about 2400 kR was found, i.e. lower than the observed value by a factor of 2. According to (7.4), the emission is proportional to k_2. If we assume a value for k_2 twice as high as the value used here, complete agreement would also be obtained for the absolute value of the intensity. However, such a high k_2-value is not very likely, since it would imply too high ozone values in the region 45—70 km (compare Figure 7).

The computed values of nighttime number densities of atomic oxygen may serve as a basis for theoretical computations of the green line ($\lambda = 5577$ Å) emission in the airglow. The excitation mechanism, proposed by CHAPMAN, is believed to be a threebody collision between oxygen atcms

$$O(^3P)+O(^3P)+C(^3P)\rightarrow O_2+O(^1S) \qquad (7.7)$$

The reaction rate of this process has been measured by YOUNG and BLACK (1965), who found a value of 2×10^{-34} cm^6/s. The resulting theoretical vertical profiles for the

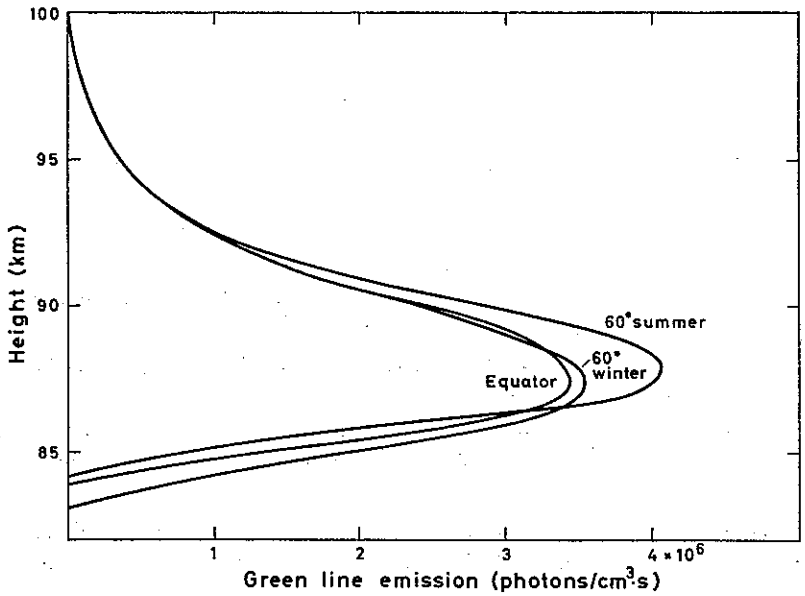

Fig. 13: Theoretical profiles for atomic oxygen green line emission in a photochemical model atmosphere with vertical eddy diffusion.

green line emission are drawn in Figure 13. The level of maximum emission is seen to be the same, 93 km, for all latitudes and seasons. On the other hand the total emission from a vertical unit column varies considerably with latitude and season. The emission was found to be 60 R for high latitudes, summer, increasing to 80 R around the Equator and to 170 R in high latitudes, winter. These figures are a little lower than the observed global mean value of about 200 R. The disagreement with observations should not, however, be considered as serious. In the first place the accuracy of the value of the reaction rate for the CHAPMAN reaction (7.7) is hardly more than within a factor of 2. Secondly, the intensity depends on the cube of the atomic oxygen number density. A 25% increase in this quantity would give complete agreement as far as the global mean value is concerned. The model predicts an annual variation which is not reflected in the observations. But here it must be emphasized that our model atmosphere is too crude for conclusions to be drawn about annual variations. Only little confidence is claimed for the accuracy of the eddy diffusion coefficients used; furthermore, horizontal transport may eliminate much of the latitudinal variation of the green line emission. But it is important to note that the results support in a convincing way the assumption that the CHAPMAN reaction is the most important excitation mechanism for atomic oxygen in the lower thermosphere.

8. Acknowledgements. I am indebted to cand.real. HARALD DOVLAND for stimulating discussions and assistance with programming. I must also thank cand.real. IVAR ISAKSEN and cand.real. PER REISO for assistance with programming.

The research reported in this paper has been sponsored by United States' Army through its European Research Office under contract number DAJA 37-67-C-0848.

REFERENCES

BAKER, D. J., 1967: Radiative exchange mechanisms. Contract no. AF 19(628)–5916. Quarterly Status Report no. **3**, 1. April 1967. Utah State University, Logan, Utah.

BATES, D. R., and M. NICOLET, 1950: The photochemistry of atmospheric water vapor. *J.Geophys.Res.*, **55**, pp. 301–327.

BENSON, S. W., and A. E. AXWORTHY, 1965: Reconsiderations of the rate constants from the thermal decomposition of ozone. *J.Chem.Phys.*, **42**, pp. 2614–2615.

CHAMBERLAIN, N. W., and C. A. SMITH, 1959: On the excitation rates and intensities of OH in the airglow. *J.Geophys. Res.*, **64**, 0pp. 611–614.

CHAMPION, K. S. W., 1967: Variations with season and latitude of density, temperature and composition in the lower thermosphere. *Space Research VII*, **2**, pp. 1101–1108.

CLYNE, M. A. A., and B. A. THRUSH, 1963: Rates of elementary processes in the chain reaction between hydrogen and oxygen, 2. Kinetics of the reaction of the reaction of hydrogen atoms with molecular oxygen. *Proc. Roy.Soc.*, London, A, **275**, pp. 559–566.

COLE, A. E., and A. J. KANTOR, 1963: Air Force interim supplemental atmospheres to 90 km. *A.F.Surv. in Geoph.*, no. 153, December 1963. (Also in *Handbook of Geophysics and Space Environments*, McGraw-Hill, 1965).

DE MORE, W. B., and O. F. RAPER, 1964: Deactivation of $O(^1D)$ in the atmosphere. *Astrophys.Journ.*, **139**, pp. 1381–1383.

FENIMORE, C. P., and C. W. JONES, 1958: Determination of hydrogen atoms in rich, flat, premixed flames by reaction with heavy water. *J.Phys.Chem.*, **65**, pp. 993–995.

FITZSIMMONS, R. V., and E. J. BAIR, 1964: Distribution and relaxation of vibrationally excited oxygen in the flash photolysis of ozone. *J.Chem.Phys.*, **36**, pp. 2681–2692.

FONER, S. N., and R. L. HUDSON, 1962: Mass spectrometry of the HO_2 free radical. *J. Chem.Phys.*, 36, pp. 2681–2692.

FRIEDMAN, H., 1961: Lyman-*a* radiation. *Ann. de Géophys.*, **17**, pp. 30–33.

HAMPSON, J., 1964: Photochemical Behavior of the Ozone Layer. Canadian Armament Research and Development Establishment. T.N., 1627/64.

— 1966: Chemiluminescent emissions observed in the stratosphere and mesosphere. In *Les problèmes Météorologiques de la Stratosphère et de la Mésosphère*, Presses Universitaires de France, Paris 1966.

HEPPNER, J. P., and L. H. MEREDITH, 1958: Nightglow emission altitudes from rocket measurements. *J.Geophys. Res.*, **63**, p. 51.

HESSTVEDT, E., 1964: On the water vapor content in the high atmosphere. *Geofys.Publ.*, **25**, no. 3, pp. 1–18.

1965: On the dependence of the intensity of the green line emission on atmospheric motion. Paper presented at Symposium on Interactions between the Upper and Lower Layers of the Atmosphere, Vienna, May 1966. (unpublished)

HUNT, B. G., 1966: Photochemistry of ozone in a moist atmosphere. *J. Geophys.Res.*, **71**, no. 5, pp. 1385–1398.

JOHNSON, F. S., J. D. PURCELL, R. TOUSEY, and K. WATANABE, 1952: Direct measurements of the vertical distribution of atmospheric ozone to 70 kilometers altitude. *J. Geophys.Res.*, **57**, pp. 157–176

JOHNSON, F. S., and E. M. WILKINS, 1965: Thermal Upper Limit on Eddy Diffusion in the Mesosphere and Lower Thermosphere. *J.Geophys.Res.*, **70**, pp. 1281–1284, p. 4063.

KAUFMAN, F., 1964: Aeronomic reactions involving hydrogen, a review of recent laboratory studies. *Ann. de Géophys.*, **20**, pp. 106–114.

KELLOGG, W. W., 1961: Chemical heating above the polar mesopause in winter. *J.Meteor.*, **18**, pp. 373–381.

KONACHENOK, V. N., 1967: A model of an oxygen-hydrogen mesosphere. *Atmospheric and Oceanic Physics*, **3**, pp. 129–133.

KONDRATYEV, K. Y., I. Y. BADINOV, S. D. ANDREEV, V. B. LIPATOV, and V. N. KONASHYONOK, 1966: Stratospheric water vapor distribution and the problem of noctilucent clouds. Paper presented at International NLC Symposium in Tallin, March 1966.

LARKIN, F. S., and B. A. THRUSH, 1964: Recombination of hydrogen atoms in the presence of atmospheric gases. *Discussions Faraday Soc.*, **37**, p. 113.

LOWE, R. P., 1960: Canadian Armament Research and Development Establishment. *Tech.Memo.* 291/59. (May 1960).

MASTENBROOK, H. J., 1968: Water vapor distribution in the stratosphere and high troposphere. *J. Atmos. Sci.*, **25**, pp. xx–xx.

MURGATROYD, R. J. and R. M. GOODY, 1958: Sources and sinks of radiated energy from 30 to 90 km. *Quart.J.Roy.Meteorol.Soc.*, **84**, pp. 225–234.

NIER, A. O., J. H. HOFFMAN, C. Y. JOHNSON, and J. C. HOLMES, 1964: Neutral composition of the atmosphere in the 100- to 200 kilometer range. *J.Geophys.Res.*, **69**, pp. 979–989.

PACKER, D. M., 1961: Altitudes of the night airglow radiations. *Ann. de Géophys.*, **17**, 67–75.

PETTERSEN, H. L., and C. B. KRETCHMER, 1960: Kinetics of recombination of atomic oxygen at room temperature. U.S. Department of Commerce, O.T.S., A.D. 283044.

RAWCLIFFE, R. D., G. E. MELROY, R. M. FRIEDMAN, and E. H. ROGERS, 1963: Measurements of vertical distributions of ozone from a polar orbiting satellite. *J.Geophys.Res.*, **68**, pp. 6425–6429.

REEVES, R. R., G. MANELLA, and P. HARTECK, 1960: Rate of recombination of oxygen atoms. *J.Chem. Phys.*, **32**, pp. 632–633.

SCHAEFER, E. J., and M. H. NICHOLS, 1964: Upper air neutral composition measurements by a mass spectrometer. *J.Geophys.Res.*, **69**, pp. 4649–4660.

SCHIFF, H. I., 1967: Private communication.

SCHUMB, W. C., C. N. GATTERFIELD, and R. L. WENTWORTH, 1955: *Hydrogen Peroxide.* Reinhold Publishing Corporation, N.Y., 1955, p. 287.

TARASOVA, T. M., 1961: Astr.Circ., U.S.S.R., no. 222, p. 31.

THOMPSON, B. A., P. HARTECK, and R. R. REEVES JR., 1963: Ultraviolet absorption coefficients of CO_2, CO, O_2, H_2O, N_2O, NH_3, NO, SO_2 and CH_4 between 1850 and 4000 A. *J.Geophys.Res.*, **68**, pp. 6431–6436.

WATANABE, K., 1958: Ultraviolet absorption processes in the upper atmosphere. *Adv. in Geophys.*, **5**, pp. 153–221.

YOUNG, C. and E. S. EPSTEIN, 1962: Atomic oxygen in the polar winter mesosphere. *J.Atmos.Sci.*, **19**, pp. 435–443.

YOUNG, R. A. and G. BLACK, 1965: Excitation of the auroral green line in the earth's nightglow. *Planetary and Space Science*, **14**, pp. 113–116.

Avhandlinger som ønskes opptatt i «Geofysiske Publikasjoner», må fremlegges i Videnskaps-Akademiet av et sakkyndig medlem.

Vol. XXII.

No. 1. L. Harang and K. Malmjord: Drift measurements of the E-layer at Kjeller and Tromsø during the international geophysical year 1957—58. 1960.
» 2. Leiv Harang and Anders Omholt: Luminosity curves of high aurorae. 1960.
» 3. Arnt Eliassen and Enok Palm: On the transfer of energy in stationary mountain waves. 1961.
» 4. Yngvar Gotaas: Mother of pearl clouds over Southern Norway, February 21, 1959. 1961.
» 5. H. Økland: An experiment in numerical integration of the barotropic equation by a quasi-Lagrangian method. 1962.
» 6. L. Vegard: Auroral investigations during the winter seasons 1957/58—1959/60 and their bearing on solar terrestrial relationships. 1961.
» 7. Gunnvald Bøyum: A study of evaporation and heat exchange between the sea surface and the atmosphere. 1962.

Vol. XXIII.

No. 1. Bernt Mæhlum: The sporadic E auroral zone. 1962.
» 2. Bernt Mæhlum: Small scale structure and drift in the sporadic E layer as observed in the auroral zone. 1962.
» 3. L. Harang and K. Malmjord: Determination of drift movements of the ionosphere at high latitudes from radio star scintillations. 1962.
» 4. Eyvind Riis: The stability of Couette-flow in non-stratified and stratified viscous fluids. 1962.
» 5. E. Frogner: Temperature changes on a large scale in the arctic winter stratosphere and their probable effects on the tropospheric circulation. 1962.
» 6. Odd H. Sælen: Studies in the Norwegian Atlantic Current. Part II: Investigations during the years 1954—59 in an area west of Stad. 1963.

Vol. XXIV.

In memory of Vilhelm Bjerknes on the 100th anniversary of his birth. 1962.

Vol. XXV.

No. 1. Kaare Pedersen: On the quantitative precipitation forecasting with a quasi-geostrophic model. 1963.
» 2. Peter Thrane: Perturbations in a baroclinic model atmosphere. 1963.
» 3. Eigil Hesstvedt: On the water vapor content in the high atmosphere. 1964.
» 4. Torbjørn Ellingsen: On periodic motions of an ideal fluid with an elastic boundary. 1964.
» 5. Jonas Ekman Fjeldstad: Internal waves of tidal origin. 1964.
» 6. A. Eftestøl and A. Omholt: Studies on the excitation of N_2 and N_2^+ bands in aurora. 1965.

Vol. XXVI.

No. 1. Eigil Hesstvedt: Some characteristics of the oxygen-hydrogen atmosphere. 1965.
» 2. William Blumen: A random model of momentum flux by mountain waves. 1965.
» 3. K. M. Storetvedt: Remanent magnetization of some dolerite intrusions in the Egersund Area, Southern Norway. 1966.
» 4. Martin Mork: The generation of surface waves by wind and their propagation from a storm area. 1966.
» 5. Jack Nordø: The vertical structure of the atmosphere. 1965.
» 6. Alv Egeland and Anders Omholt: Carl Størmer's height measurements of aurora. 1966.
» 7. Gunnvald Bøyum: The energy exchange between sea and atmosphere at ocean weather stations M, I and A. 1966.
» 8. Torbjørn Ellingsen and Enok Palm: The energy transfer from submarine seismic waves to the ocean. 1966.
» 9. Torkild Carstens: Experiments with supercooling and ice formation in flowing water. 1966.
» 10. Jørgen Holmboe: On the instability of stratified shear flow. 1966.
» 11. Lawrence H. Larsen: Flow over obstacles of finite amplitude. 1966.

Vol. XXVII.

No. 1. Arne Grammeltvedt: On the nonlinear computational instability of the equations of one-dimensional flow. 1967.
» 2. Jørgen Holmboe: Instability of three-layer models in the atmosphere. 1968.
» 3. Einar Høiland and Eyvind Riis: On the stability of shear flow of a stratified fluid. 1968.

A.s John Griegs Boktrykkeri